

The Genomic Landscape of Oceania

Consuelo D. Quinto-Cortés^{*1}, Carmina Barberena Jonas^{*1}, Sofía Vieyra-Sánchez^{*1}, Stephen Oppenheimer², Ram González-Buenfil¹, Kathryn Auckland³, Kathryn Robson², Tom Parks², J. Víctor Moreno-Mayar⁴, Javier Blanco-Portillo⁵, Julian R. Homburger⁵, Genevieve L. Wojcik⁶, Alissa L. Severson⁵, Jonathan S. Friedlaender⁷, Francoise Friedlaender⁷, Angela Allen⁸, Stephen Allen^{8,9}, Mark Stoneking^{10,11}, Adrian V. S. Hill², George Aho¹², George Koki¹³, William Pomat¹³, Carlos D. Bustamante⁵, Maude Phipps¹⁴, Alexander J. Mentzer^{2,}, Andrés Moreno-Estrada^{1,**}, and Alexander G. Ioannidis^{15,**}**

¹National Laboratory of Genomics for Biodiversity (LANGEBIO)—Advanced Genomics Unit, CINVESTAV, Mexico

²University of Oxford, UK

³Department of Medicine, University of Cambridge, UK

⁴Centre for GeoGenetics, University of Copenhagen, Denmark

⁵Stanford University, USA

⁶Johns Hopkins Bloomberg School of Public Health, USA

⁷Department of Anthropology, Temple University, USA

⁸Edward Francis Small Teaching Hospital, Republic of The Gambia

⁹Liverpool School of Tropical Medicine, UK

¹⁰Department of Evolutionary Genetics, Max Planck Institute for Evolutionary Anthropology, Germany

¹¹Centre National de la Recherche Scientifique, France

¹²Vaiola Hospital, Tonga

¹³Papua New Guinea Institute of Medical Research, Papua New Guinea

¹⁴Jeffrey Cheah School of Medicine and Health Sciences, Monash University Malaysia, Malaysia

¹⁵Department of Biomolecular Engineering, University of California Santa Cruz, USA

^{*}These authors contributed equally

^{**}Correspondence: alexander.mentzer@ndm.ox.ac.uk, andres.moreno@cinvestav.mx, ioannidis@ucsc.edu

May 12, 2024

Abstract

Encompassing regions that were amongst the first inhabited by humans following the out-of-Africa expansion, hosting populations with the highest levels of archaic hominid introgression, and including Pacific islands that are the most isolated inhabited locations on the planet, Oceania has a rich, but understudied, human genomic landscape. Here we describe the first region-wide analysis of genome-wide data from population groups spanning Oceania and its surroundings, from island and peninsular southeast Asia to Papua New Guinea, east across the Pacific through Melanesia, Micronesia, and Polynesia, and west across the Indian Ocean to related island populations in the Andamans and Madagascar. In total we generate and analyze genome-wide data from 981 individuals from 92 different populations, 58 separate islands, and 30 countries, representing the most expansive study of Pacific genetics to date. In each sample we disentangle the Papuan and more recent Austronesian ancestries, which have admixed in various proportions across this region, using ancestry-specific analyses, and characterize the distinct patterns of settlement, migration, and archaic introgression separately in these two ancestries. We also focus on the patterns of clinically relevant genetic variation across Oceania—a landscape rippled with strong founder effects and island-specific genetic drift in allele frequencies—providing an atlas for the development of precision genetic health strategies in this understudied region of the world.

Introduction

Oceania (including Micronesia, Melanesia, and Polynesia) has had a complex demographic history, with human settlements in Papua New Guinea dated over 50,000 years ago¹ and migrations out across the Polynesian archipelagos continuing through relatively recent times, including the Lapita expansion (3500 - 3000 BP) reaching Tonga and Samoa, and culminating in the settlement of eastern Polynesia (1500 - 1000 BP)^{2,3}. Melanesia mainly refers to coastal New Guinea and the nearby islands such as the Solomon Islands, Fiji, and Vanuatu. Micronesia is a group of islands that are north of Melanesia and west of Polynesia, and contains such regions as the Marshall Islands, Palau, Guam, and Nauru. Polynesia indicates the easternmost and most remote islands in the Pacific, such as Tonga, Samoa, the Marquesas, and the Cook Islands. Most Micronesian and Polynesian languages are from the Oceanic branch of the Malayo-Polynesian group of the Austronesian language, with the notable exceptions in Micronesia of Palauan and Chamorro^{2,4}. This language family spanned the largest area in the world before the colonial spread of European languages, encompassing neighboring regions included in this study from the Philippines and island southeast Asia to peninsular southeast Asia and across the Indian Ocean to Madagascar.

Oceania is of particular interest given the occurrence of Denisovan introgression in human populations of the Pacific. There is strong evidence of Denisovan admixture in the Philippines and Papua New Guinea, but their contribution to the genetic makeup of other populations in Oceania has not been fully determined^{5,6}. Although several populations from Oceania have been previously studied using classical and uniparental markers⁷⁻¹⁰ and more recently, a few sub-regions have been investigated using genome-wide and whole genome data¹¹⁻¹³, there is still a large gap in our knowledge of pan-Oceania connections and the overall genetic diversity of this vast region as a whole, which surely impacts the development of personalized medicine for the benefit of individuals from this region spanning more than 30 nations. Also, the extent and impact of the different modern and archaic human migrations that might have occurred in the area are still unresolved. In order to assess these questions, we performed analyses into patterns of genetic diversity and relatedness in modern samples and ancient samples, characterized the archaic introgression in these populations, and examined variants of potential clinical relevance in this dataset.

Results and Discussion

Genetic variation in the Pacific and zones of transitions

First, we explored the patterns of region-wide genetic variation in our dataset. The clusters of population differentiation identified by unsupervised clustering¹⁴ broadly correspond to Melanesia, Micronesia, and Polynesia, thus reflecting the cultural and linguistic differences amongst these regions (Figure 1B, K=9). We observed a gradient of East Asian like ancestry (orange color) that decreased eastward from the mainland. This gradient could be a combination of both historic relationships, such as seafaring trade throughout the Indonesian archipelago, and modern admixture events. Notably, the indigenous groups from the southern Philippines (Mamanwa and Manobo) do not share this component, and instead have ancestry components observed mainly in Micronesia, Melanesian, and Polynesian individuals.

In the populations from Melanesia, we found two distinct major genetic components; one particularly present in Papua New Guinea and the second in the Bismarck Archipelago and Solomon Islands. The first component comprises all of the genetic ancestry of the Highlands populations of Papua New Guinea, which are known to have very limited contact with other populations¹².

We also observe a major genetic cluster in the sampled populations from Micronesia, except for Palau and Guam, which have East Asian like ancestry. Individuals from Guam have a significant proportion of ancestry shared with East and Southeast Asian samples, and some shared with European samples. This reflects the demographics of Guam, which has a significant Filipino and European population. In Palau, there is also an important East Asian component likely representing the contribution from Malay and Filipino admixture. However, it is difficult to disentangle modern and ancient signals of southeast Asian admixture in Palau. Its language is classified in a different subgroup, Western Malayo-Polynesian, than much of the rest of Micronesia, which are classified as Oceanic languages². The Western Malayo-Polynesian subgroup is spoken in many regions of the Philippines and Indonesia today and this may reflect much closer ties to those regions throughout history⁴.

In Polynesia, the genetic ancestry clustering patterns seen in the westernmost islands (Tonga and Samoa) contrast with those seen in the rest of the Polynesian islands as they contain both of the components seen in Polynesia and in Melanesia. This pattern likely indicates the recent founder effect that occurred during the settlement of many of these archipelagos, with the easternmost Polynesian islands being more directly related to each other, anchoring this clustering component. This is consistent with the hypothesis that the historical homeland of the Polynesian cultures was located in the region of Tonga and Samoa from which individuals migrated out to the more eastern Polynesian islands in the last two millennia^{2,15}. We also observe signals of modern European admixture, especially in Guam, Palau, and Polynesia, that are the genetic evidence of the colonization from Spain and other western European countries^{16,17} (shown as dark blue component in Figure 1B and Supplementary Figure 3). Many islands in Polynesia, especially the South Marquesas and Palliser Islands, also possess a small ancestry percentage similar to Indigenous American populations, this is consistent with the hypothesis of the Native American contact with Polynesia¹⁸.

Our dataset, while primarily centered on Oceania, also incorporates data from four distinct populations in Madagascar. This inclusion is centered on Madagascar's unique history combining African and Austronesian heritage. Consistent with this dual heritage, the four Malagasy populations featured in our study display markers of both African and East Asian ancestries. This genetic intermingling is visually represented in 1B, where African ancestry is depicted with a red component and East Asian ancestry with an orange component¹⁹.

The Principal Component Analysis (PCA) results reveal that the population variation is primarily distributed among three clusters: one composed mainly of the Melanesian samples, including the Papuan Highlanders at one extreme; another containing the Polynesian samples and a third with samples from Taiwan and southeast Asia. Micronesian samples, on the other hand, are found in the space defined by these main clusters (Figure 2A).

Within the Melanesian cluster, the East Sepik and Highlander populations from Papua New Guinea are the furthest separated, while Russell is closer to the Polynesian cluster, and Ontong Java and Tikopia group towards the mainland southeast Asia and Taiwan clusters. We also identify outliers in the Micronesian cluster, where Kiribati, Tuvalu and Kapingamarangi group with the Polynesian samples, and an individual from the Republic of Nauru, is grouped towards the Melanesian cluster. Interestingly, the indigenous Mamanwa and Manobo populations in the Philippines are more closely grouped with the Polynesian and Melanesian clusters, in contrast to other Filipino populations that are more closely associated with the Southeast Asian cluster.

As the Lapita culture had a significant influence in the Pacific, we included eight ancient samples from Lapita sites located in Vanuatu and Tonga²⁰⁻²² in the PCA and ancestry specific tree analyses. In the PCA, the ancient samples form their own cluster and do not overlap with their present-day equivalents. This difference could be due to recent migrations and admixture events in Vanuatu and Tonga.

Figure 2B depicts the relationships among populations in our dataset using only genomic variant sites in East Asian chromosomal segments as identified by a local ancestry analysis. Here, generally, populations group according to their geographical affiliation. First, there is a clade comprising populations from mainland southeast Asia, along with the Andamanese and Tenggerese. The four populations from Madagascar form a separate clade. Next, the populations from Northern Philippines cluster with Alor. Following that branching, we observe the rest of the island southeast Asia, with the exception of Russell, Mendi and Tikopia. The Aboriginal Taiwanese form a distinct clade, where Ami appears to be an outgroup to the other populations. Three primary clades can be observed in Melanesia: one comprising Papua New Guinea, another the smaller islands of Melanesia, and a third one with the Bismarck archipelago and the Solomon Islands. The next clade mainly consists of samples from Micronesia, with outliers Palau and Guam as outgroups to the island southeast Asia clade. Finally, there is a large clade with all Polynesian populations from this study. Interestingly, the ancient Lapita samples are located in the same node as New Caledonia, where the first Lapita cultural remains were discovered, in the Austronesian ancestry-specific tree, and are in the same clade as the Polynesian samples, Mamanwa and Manobo, Fiji and Bank and Torres. Populations from the most eastern islands appear to be more closely related and have diverged most recently.

Recent migration into the Philippines

Identity by Descent (IBD) estimation is a powerful tool for identifying populations and individuals with shared genetic ancestry, allowing for the detection of past and recent migrations as well as population relationships.

As we move eastward across Oceania, we observe an increase in the amount of shared IBD between different populations, with the highest levels of IBD observed among Polynesian populations, particularly those in the easternmost islands (Figure 3A). This pattern is consistent with very recent settlement and a shared bottleneck (or series of bottlenecks) due to settlement by a small founder group. In contrast, Melanesia has lower levels of IBD than both Polynesia and Micronesia, which correlates with the greater cultural and linguistic diversity in Melanesia and much deeper age of settlement (Figure 3B).

Within Polynesia, there is a clear split between West and East, with Polynesian populations on the smaller Eastern islands showing higher values of IBD sharing than those in the more western isles of Tonga and Samoa (Figure 3A). This is consistent with archaeological records suggesting that the founding populations of eastern Polynesia came from these western islands, as well as cultural evidence suggesting higher effective population sizes in general in the western region of Polynesia. This ancestry split mirrors differences in cultural practices and languages between Polynesian islands.

Previous studies have noted that Pacific islander populations derive much of their ancestry from two different ancestral groups: individuals who settled island southeast Asia over 50,000 years ago and form the predominant genetic ancestry component of islands like New Guinea and a second recent group more closely related to East Asian populations, specifically indigenous populations in Taiwan. We refer to the former genetic ancestry as Papuan, reflecting the largest island that is dominated by it, and the latter as Austronesian, reflecting the language family spoken by most of the groups possessing a majority component of this ancestry. The admixture between these two groups led to the formation of most modern Oceanian populations, although some groups have only Papuan ancestry (highland New Guinea) or only Austronesian (indigenous Taiwan) while other groups have additional ancestry components as well (such as colonial European ancestry in Polynesia and African ancestry in Madagascar). Polynesian and Micronesian populations share IBD with populations from island Melanesia and the Southern Philippines (Mamanwa and Manobo) (Figure 3A), consistent with sharing ancestry from both groups. This pattern is also observed in the PCA, ADMIXTURE plots and NJ tree (Figures 1B and 2A), supporting the hypothesis that significant admixture occurred. The timing and extent of this admixture event has not been studied, and so we formally tested the relationship between Taiwan, the Southern Philippines (Mamanwa and Manobo) and Northern Philippines (Agta and Aeta) and the rest of the Oceanian populations with the f_3 statistic (Figures 3 and S10).

When we tested $f_3(A, \text{Mamanwa and Manobo}; \text{Yoruba})$, specifically with Polynesian and Micronesian populations as test populations A, we observed higher positive values, implying close relatedness between these populations and Mamanwa and Manobo. We then estimated IBD decay lambda and psi statistics¹⁵ with the populations that shared equal to or more than 20 cM with Mamanwa and Manobo (Figures 4 and S11).

Drawing on the comprehensive evidence linking the Mamanwa and Manobo populations to the Pacific, we investigated the directionality of this migration. To address this, we employ the directionality index (ψ), a measure that quantifies the aggregate increase in frequencies of retained rare variants across the genome due to founder events, thereby elucidating the trajectory of range expansion¹⁵. This statistical approach enables us to delineate the parental population from its descendants. We calculated the pairwise ψ for Mamanwa and Manobo against each of the 13 populations exhibiting the strongest IBD signals (>20cM) with them (refer to Supplementary Figure S11). Our findings indicate a range expansion originating from Samoa and Tonga, positioning these as the ancestral islands, aligning with the established narrative of Polynesian expansion¹⁵. However, the Mamanwa and Manobo are downstream of Samoa and Tonga in this range expansion. This indicates that a reverse migration occurred of Austronesian speakers from western Polynesia back towards Asia leading to the formation of the Manobo and Mamanwa Austronesian genetic component back in the Philippines. Such long distance west-to-east Austronesian migrations in this era are not unprecedented, as another such long distance voyage is responsible for the settlement of Madagascar by Austronesia speakers.

Further, our analysis reveals a bifurcation pattern towards the east and west, with the lowest ψ values observed in Raivavae and Russell, islands farthest from Tonga and Samoa. Through the examination of the IBD segments length distributions, we uncovered more recent connections between Mamanwa and Manobo, offering deeper insights into these migration patterns. More recent migrations are characterized by longer IBD segments, in contrast to older migrations, which accumulate shorter segments. By calculating the exponential decay constants (λ), as shown

in Figures 4a and 4c, of these decay distributions, we corroborated the findings from our ψ analysis that Tonga and Samoa represent the closest connections with Manobo and Mangareva in the range expansion, followed by a bifurcation towards both the most remote parts of Polynesia and regions closer to East Asia. This pattern suggests a diverging source population from Samoa and Tonga, part of which settled in remote Polynesia while another segment experienced a reverse migration to the Philippines, the latter being ancestors of the current Manobo and Mamanwa populations. This new finding is consistent with previous indications of a potential source of ancestry from the Philippines in Polynesian individuals²³, and past interactions between populations from Island South East Asia (ISEA), Micronesia, islands north of Melanesia, and Polynesia^{24,25}.

By uncovering the migratory links between the Mamanwa and Manobo populations to the Pacific Islands, this research sheds light on the complexities of human movements and the spread of cultures across vast oceanic distances and elucidates another of the multiple waves of migration that populated the Philippine islands⁶. It challenges previous assumptions about the isolation of certain populations and reveals a more interconnected Oceanian world than previously understood, precisely at the time when some of the longest Austronesian voyages of discovery (into Polynesia and into the Indian Ocean) were taking places.

Denisovan introgression in the Pacific

The D-statistic compares the allele frequencies of different populations to detect gene flow between them²⁶. In this study, we used the topology D(Yoruba, OGVP; Denisova, Chimpanzee). A D value of zero indicates that the Oceanian and Yoruba populations are more similar to each other than to Denisova or chimpanzee, suggesting no detectable gene flow from Denisovans. Negative D-statistic values suggest more shared allele frequencies between the Oceanian population being tested and Denisova, which may be indicative of gene flow from Denisova. Our results are shown in the supplementary material (Figure S13). The signal of Denisovan introgression is primarily observed in populations from Melanesia, particularly in Papua New Guinea, and in the Agta and Aeta, two Negrito populations in the Philippines known to have a higher proportion of Denisovan introgression than other neighboring populations. Unexpectedly, we observed a strong signal of gene flow in Polynesian populations. However, the D-statistic values can be influenced by the presence of Neanderthal introgression, which is also found in the Pacific¹³. To address this, we ran an F4-ratio test using an established test topology meant to isolate Denisovan signals in Oceanians by using East Asians to control for possible confounding Neanderthal ancestry²⁷.

The F4-ratio test²⁶ is used to quantify the proportion of detectable Denisova ancestry. The ratio tested was $f_4(\text{Altai Neanderthal, Yoruba; OGVP, Han})/f_4(\text{Altai Neanderthal, Yoruba; Denisova, Han})$. We applied this to three sets of our data: using global data (non-ancestry-specific), restricting only to segments called as East Asian in our RFMix results, and then separately restricting only to segments called as Papuan in our RFMix results. Our results on global ancestry show an average of 3.2% Denisovan introgression in Papuan Highlanders, with the second-highest values found in native northern Philippines populations (Aeta and Agta) (Figure 5A). We also identify low but detectable signals of introgression in remote Oceania. The results show a clear difference between the signal detected in the Austronesian ancestry of each population and the signal detected in the Papuan ancestry. The analysis on the Papuan-specific component shows that most populations, even those in remote Oceania, have percentages of Denisovan introgression ranging from 2-5% in this component, with the highest values found in Agta and Aeta (Figure 5B). The analysis on the East Asian component, on the other hand, shows no detectable Denisovan introgression in most of the samples, except interestingly <1% in the Maumere and Tikopia (Figure 5C). The exceptions are the Agta and Aeta populations, which have almost 2% Denisovan introgression in their Austronesian component, contrasting with the low or absent signal in the rest of the samples. This Denisovan signal recovered in the East Asian component is consistent with reports of multiple pulses of Denisovan introgression into modern humans in different regions and different historical ancestries^{5,28}. Additionally, this combined contribution of the Papuan and East Asian components to the proportion of Denisovan introgression to the Negrito populations (Agta and Aeta) could be one of the reasons why other populations from the region are among the ones with highest proportion of Denisovan ancestry⁶. Additionally, we identified significant differences between the average proportions of Denisovan introgression per region when looking at global ancestry data, but this difference is not observed when looking only at the proportions obtained from Papuan ancestry (Figures 5 S12). This suggests that

differences in proportions of Papuan ancestry between regions may drive differences in proportions of Denisovan introgression, but the average proportion of Denisovan introgression within Papuan ancestry itself remains generally constant.

Distribution of variants of clinical relevance

As each island in the Pacific has a unique demographic history and underwent a founding event, it is essential to accurately profile the distribution of pharmacogenetic variant frequencies in each Oceanian population separately, even if they seem closely related in ancestry. For this purpose, we annotated the sites present in the MEGA array using ANNOVAR²⁹ and CLINVAR³⁰ and found four sites with pathogenic variants: rs2272457 (chromosome 15, gene *CHD2*), rs2297902 (chromosome 1, associated with Hypokalemic periodic paralysis 1, gene *CACNA1S*), rs237025 (chromosome 6, associated with Diabetes mellitus, gene *SUMO4*), and rs6063910 (chromosome 1, associated with Acute myeloid leukemia with maturation, gene *MIR181A1HG*). The frequency distribution of these variants in the different geographical groups can be seen in Figure S15.

We also identified four SNPs that have a role in drug response: rs6977820 (chromosome 7) and rs1954787 (chromosome 11) have been linked to adverse side effects in antipsychotics and antidepressants treatment, respectively, while rs4149056 (chromosome 12) and rs1719247 (chromosome 15) are associated with reactions to statins. In particular, the C allele of the rs4149056 locus in *SLCO1B1* is associated with an increased risk of adverse side effects, including myopathy, in patients on statins³¹. This allele's frequency does not vary considerably between regions in Oceania but exhibits higher values than in the HGDP populations (Figure S15). As the rate and treatment of heart disease and other chronic diseases increase in Oceanic populations, it will be essential to know which pharmaceutical interventions have the most efficacy.

Regarding COVID-19 infection, we found in our dataset previously reported variants by recent publications^{32,33}. In particular, rs10774671 is located in the *OAS1* gene on chromosome 12 and this gene produces an enzyme called 2'-5' oligoadenylate synthetase 1 that is important in the innate immune response. This SNP has been linked to susceptibility to infectious diseases such as COVID-19, West Nile Fever, Severe Acute Respiratory Syndrome (SARS), Hepatitis C, and multiple sclerosis³⁴⁻³⁷. The mutation G to A in the last nucleotide of intron 5 changes a splicing site and generates an isoform with a higher molecular weight and lower enzymatic activity, which affects the innate immune response against RNA viruses³⁷.

Interestingly, recent studies have linked the gene cluster containing *OAS1* along with *OAS2* and *OAS3* to severe COVID-19 infection in individuals of European ancestry who possess a protective haplotype derived from Neanderthal introgression^{38,39}. In these studies, rs10774671 was identified as the candidate causal variant, as the G allele appears to provide protection against COVID-19 hospitalization. Notably, the haplotype where rs10774671 is located is also found in Papua New Guineans with likely Denisovan origin⁴⁰. Moreover, the G allele is highly prevalent in individuals of African ancestry (58%)³⁹, which may suggest that this allele was present in the ancestral population of modern humans, Denisovans, and Neanderthals. Additionally, SNP rs1886814 in the *FOXP4* gene has also been associated with COVID-19 infection³², and it is correlated with variants causing adenocarcinoma and subclinical interstitial lung disease³². We provided the frequency distribution of the rest of COVID-19 associated SNPs in Figure S14.

On a different note, the SNP rs12513649, associated with body mass index, is observed throughout Polynesia (Figures 1C and S15). It is also present in many of the indigenous populations in the Philippines and Taiwan but it is much rarer in Papua New Guinea and Melanesia. This variant is strongly correlated with the Polynesian ancestry component ($r=0.57$, $p < 1 \times 10^{-10}$) as many Polynesian countries, including Samoa, Nauru, Cook Islands, and Tonga, have some of the highest rates of obesity in the world⁴¹. Another site, rs3008049, which is under selection in the Bajau⁴², has a wide geographic distribution but at low frequencies (~3%) (Figures 1C and S15). In our dataset, the highest frequency of this SNP was found in Melanesia. When looking at alleles of interest, BMI in Samoa and spleen size in Indonesia, we see that they are not common in only those populations, but they are instead more widespread throughout the Pacific.

These findings emphasize the importance of including data from diverse populations to achieve effective personalized medicine. As the use of genetics in clinical practice becomes more widespread, it is crucial to

understand the diverse ancestries of different populations to ensure that new and current treatments are tailored to each population's unique genetic makeup. As the majority of the clinical annotations generally come from studies in European populations, we might not have the power to find many relevant variants in our dataset, highlighting the importance of studying underrepresented populations.

Conclusion

Here we present an extensive collection of samples from the Pacific, filling a substantial gap in the worldwide representation of human populations. The Pacific is an area with diverse demographic histories, rich with migrations and admixture events. Using genome wide data, we confirmed that the islands of Tonga and Samoa define a transition zone between remote Oceania and Polynesia. We also observed that, after the arrival of the Lapita people to Tonga and Vanuatu, there has been population admixture and indeed the modern day samples from these islands do not cluster with the ancient samples; however, the ancient samples do cluster with the Austronesian component in the modern samples, showing that the ancient samples on those islands are the ancestors of the modern islanders. This contradicts a narrative that has gained traction following previous work, which asserts incorrectly that the modern inhabitants of these islands are not ancestrally indigenous to them. Interestingly, we also identified a back-migration from western Polynesia to the Philippines that has not been previously reported. This east to west migration highlights the mobility of the populations in the Pacific and contrasts with the idea of an exclusive west to east movement. We expanded the quantification of Denisova ancestry in the eastern Pacific and found that the presence of this ancestry is linked to Papuan ancestry in the area in general, but has some unique occurrences in the Austronesian ancestry. In particular, we identified possible dual sources of Denisovan introgression into both the Austronesian and Papuan ancestors of indigenous populations from the Philippines that could be a reason for their elevated Denisovan signals. Finally, we explored the geographical distribution of variants of clinical interest that show large variability in frequency across this region.

Materials and Methods

Oceanian genotype data and general quality control

981 samples from 92 populations and 30 countries in Oceania and Southeast Asia were genotyped on the MEGA-EX Illumina platform (1,895,184 markers before quality control) using the b37 (hg19) version of the human genome. We recognize that geographic classification of the Pacific might not actually represent cultural or genetical differences but for the sake of clarity, we used the following labels for the major geographic groups of our dataset: Taiwan, Mainland southeast Asia (MSEA), Island southeast Asia (ISEA), Melanesia, Micronesia and Polynesia (see Figure 1A).

For quality control purposes, we separated the samples into two groups, depending whether they have a Melanesian geographic origin ($n=347$) or not ($n=634$), to perform the following steps with PLINK 1.9⁴³:

- Remove individuals with a missing call rate greater than 10% (`--mind 0.1`)
- Exclude sites with a call rate lower than 5% (`--geno 0.05`)
- Flip alleles at sites that differ from the human reference genome b37.
- Calculate relatedness (r , `--genome`) between all pairs of individuals to find and remove one member of the related pairs with r greater than 0.25
- Filter SNPs with a Hardy-Weinberg equilibrium exact test p-value below $1e-8$ (`--hwe 1e-8`)

Finally, we removed duplicated variants. The final working dataset (OGVP) contains 913 individuals and 1,797,365 SNPs.

Datasets description

For the analyses that required continental references, we used the following individuals from the Human Genome Diversity Project (HGDP) panel genotyped in the MEGA platform⁴⁴:

- America: Surui ($n=10$), Karitiana ($n=18$), Colombian ($n=9$), Puno ($n=20$)
- Europe: French ($n=28$), Italian ($n=12$), Tuscan ($n=7$)

- Africa: Bantu (South Africa/Kenya) (n=19), Mandenka (n=22), San (n=60), Yoruba (n=22)
- East Asia: Cambodian (n=10), Dai (n=10), Han (including Northern Han Chinese) (n=44), Japanese (n=29), Lahu (n=8), Naxi (n=9)
- South Asia: Sindhi (n=24), Kalash (n=23)

We also built a panel of ancient DNA samples from the geographic areas of interest that was merged with our panel of present-day samples. Finally, we generated another dataset with the OGVP samples and whole genome sequences from Altai Neanderthal⁴⁵, Altai Denisova⁴⁶ and the chimpanzee⁴⁷ to look at possible introgression from these hominins in the Pacific.

See Table S1 for the detailed information of the samples used in this study.

Patterns of genetic diversity

Since linkage disequilibrium affects Principal Component Analysis (PCA) and genetic clustering methods, we pruned the OGVP dataset with `PLINK --indep-pairwise 50 5 0.8`. We performed a PCA with our modern and ancient samples using the projection option of the tool `smartpca` part of AdmixTools²⁶. We projected the ancient samples onto the modern samples and enabled the flag `lsqproject` to consider the large amounts of missing data present in the ancient samples (Figure 2A).

We followed the same procedure to perform a PCA with the modern data and archaic data from Altai Neanderthal and Altai Denisova and the chimpanzee (Figure ??).

Additionally, we used the program ADMIXTURE¹⁴ to determine genetic clusters and calculated probable ancestries with K values from 2 to 17. We ran 10 replicates of each of these K values to perform a cross-validation and find the best fitting K value, and used `pong`⁴⁸ to identify the most representative replicate (Figures 1B and S3). Using the Fst values calculated by ADMIXTURE at K=9 between the inferred clusters, we built a Neighbor-Joining tree with the R function `nj`.

We also calculated the population pairwise Fst with `smartpca`; the results can be seen in the supplementary material (Figure S6).

Ancestry specific analyses

In order to identify local ancestry segments in our samples, the haplotypes were first phased with the program SHAPEIT2⁴⁹ and then we used the software RFMix v1.5.4⁵⁰. For this particular analysis, we defined four different ancestries: African, European, Papuan and East Asian. The last two groups were made up with populations from the OGVP dataset:

- Papuan: Kundiawa, Tari, Mendi, Bundi, Marawaka, Enga, Western and Eastern Highlands
- East Asian: Atayal, Paiwan, Bunum, Ami, Igorot, Vietnamese, Han and Dai

We supported the choice of these four ancestries as seen in the ADMIXTURE plot at K=4 (Figure S3). We use the term “Papuan” to specify the genetic ancestry principally seen in Papuan New Guinea (PNG) and other parts of Melanesia and that reaches 100% in our Highlander samples. The “East Asian” ancestry refer to the ancestry seen in the majority of our Oceanic populations but which geographical origin we cannot identify.

Patterns of genetic relatedness

We identified identity-by-descent (IBD) segments with `refinedIBD`⁵¹ on the OGVP phased data. We followed the authors recommendations to merge short IBD segments, fill in and remove gaps between IBD segments with at most one discordant homozygote site and that are less than 0.6 cM in length. After merging, we kept only IBD segments with length > 3 cM and looked for any segments that would overlap with regions of low complexity (namely telomeres and centromeres). We summed the length of shared IBD regions over all pairs of individuals in each population and built an IBD sharing network with the `ggplot` R package. Furthermore, we calculated the sum of IBD sharing within OGVP populations, comparing the values to the reference populations from HGDP (Figure S9).

To investigate further the genetic relationships between all the Oceanic populations and Taiwan and the Philippines, we utilized the f3 statistic using the tool `qp3Pop` part of the AdmixTools²⁶, with the flag `outgroupmode`.

This statistic is used to measure the differences in allele frequency in test populations (A and B) in reference to an outgroup (C): $f_3(A, B; C)$. In this case, we considered the Aboriginal Taiwanese (Atayal, Paiwan, Bunum and Ami), Southern Philippines (Mamanwa and Manobo) and Northern Philippines (Agta and Aeta) as test populations B against all OGVP populations as test populations A and Yoruba as the outgroup C.

In an effort to estimate the order of contact between island population, we used a previously published method that uses the shape of the distribution of shared IBD segments between all pairs of individuals of different island populations¹⁵. For each pair of islands A and B, we pooled all of the IBD segments shared between individuals on A paired with individuals on B, and fitted an exponential curve to the resulting segment length distribution (Figure 4A). We only focused on populations that shared ≥ 20 cM with Mamanwa and Manobo and estimated λ and ρ statistics¹⁵ (Figure 4B and 4C).

Comparison with ancient DNA

In the case of the ancient samples from the Pacific, we focused on eight samples identified as part of the Lapita culture in Tonga and Vanuatu (see Table S2). We computed the allele frequencies for all the SNPs present in at least one of the ancient samples (141,425 sites) and separated the samples according to their geographic origin: Lapita-Vanuatu (MAL006, I5951, I1369, I1368 and I1370)^{20,22} and Lapita-Tonga (TON001, TON002 and CP30)^{20,22}.

To estimate the population divergence between the modern and the ancient Lapita samples, we calculated the average pairwise differences (π) between the Lapita samples frequencies and the ones from the Oceanian populations. We then took an ancestry specific approach where we only considered sites from the modern samples that had an East Asian ancestry as previously defined with RFMix and we then calculated all the possible pairwise differences between the populations to generate an ancestry specific neighbor joining tree using the `bionj` function part of the `ape` R package⁵² (Figure 2B).

Comparison with archaic DNA

We used the program `snppflip` to flag any reversed or ambiguous sites in the HGDP, OGVP, and archaic files (both Neanderthal and Denisova). We flipped all the reversed sites and removed all of the ambiguous SNPs using PLINK (`--flip` and `--exclude`). We then kept only-biallelic sites in the human datasets (OGVP and HGDP), and merged them on those sites. Then, we extracted the reference allele for the chimpanzee at those sites, excluded the sites with no reference allele available, removed triallelic sites between the chimpanzee and the human dataset, and created a new file with the chimpanzee reference and the human data. Finally, we extracted the sites in this merge from the archaic hominin data, removed triallelic sites, and created a final merged file. The result was a dataset containing the information of OGVP, HGDP, Neanderthal, Denisova and the chimpanzee reference genome at sites where we had data for the chimpanzee and excluding any triallelic sites.

First, we performed a PCA with the chimpanzee, Altai Neanderthal, and Altai Denisova data, and then projected the OGVP samples on the space defined by the first two PCs using the `lsqproject` option of `smartpca` as done in Larena et. al (2021)⁶. The samples that cluster closer to the Denisovan are those from Melanesia and Aeta and Agta from the Philippines (Figure ??).

Given the known presence of Denisova introgression in Papua New Guinea⁵, we were interested in examining if this presence spread further east in the Pacific. For this purpose, we applied the D and f4-ratio using FrAnTK⁵³ to test the presence and quantify the hominin introgression in our dataset. The D-statistic is a formal test of admixture and can provide information about the directionality of gene flow²⁶. In this case, we used the test $D(\text{Yoruba}, \text{OGVP}; \text{Denisova}, \text{Chimpanzee})$ (Figure S13). The f4-ratio allows the estimation of the mixing contributions of an admixture event²⁶. We used the test $f_4(\text{Altai Neanderthal}, \text{Yoruba}; \text{OGVP}, \text{Han})/f_4(\text{Altai Neanderthal}, \text{Yoruba}; \text{Denisova}, \text{Han})$, designed to isolate Denisovan signals in populations that are also to have Neanderthal introgression²⁷ (Figure 5A).

We then quantified the proportion of Denisovan ancestry in ancestry-specific (AS) data determined by our RFMix results. From the non-ancestry-specific (nonAS) dataset, we extracted the populations to be used as references for this analysis (Yoruba, Han, Dai, Neanderthal, and Denisova). Then, we obtained the sites available for both the AS and nonAS data and extracted those sites from both datasets. Once we were working with the same sites in both datasets, the nonAS dataset, which was in PLINK format, was used to build a FrAnTK⁵³ dataset. The `pop` and `freqs`

files were then edited to add in the AS data (East Asian and Papuan ancestries), in separate merges (the chrs and regions files remained unchanged since they only contain data relating to the sites in the dataset, which are the same for both datasets in this case), resulting in two FrAnTK datasets: one containing a merge of the East Asian AS OGVP data and the nonAS references and a second merge of the Papuan AS OGVP data and the nonAS references. An f_4 -ratio analysis was then applied to these datasets to obtain ancestry-specific estimations of Denisova introgression in the populations (Figure 5B,C).

Having identified the proportions of Denisovan introgression, we determined whether the differences in the proportions of Denisovan introgression were significantly different between regions. For this purpose, we performed two-tailed t-tests for each pair of regions. We looked both at the proportions of Denisova introgression obtained when looking at global ancestry, and at those obtained from looking at Papuan ancestry data. When studying proportions obtained from global data, there were significant differences in most comparisons (Figure S12A). The largest difference was identified when comparing the proportions in Melanesia with those in Micronesia or Polynesia, but all comparisons had p-values <0.01 , except for Micronesia against Polynesia. On the other hand, when studying proportions obtained from Papuan ancestry data, we observed no statistically significant regional differences (Figure S12B).

Variants of clinical relevance

Understanding the patterns of clinical variation in the context of genetic ancestry is especially important for improving medical practice and implementing precision medicine in diverse under-represented populations. For this purpose, we looked for variants present in the MEGA array with known specific effects on health, examined the frequency of the effect alleles in our data and in the HGDP populations we previously used as continental references. We first used the tool ClinVar³⁰ and ANNOVAR²⁹ to annotate and find variants with pathogenic alleles. We then focused on two SNPs. The first one is rs12513649, located in chromosome 5, which is strongly associated with body mass index (BMI) in Samoan populations⁵⁴. The second SNP is rs3008049 in chromosome 6 is associated with hypothyroidism in the UK Biobank according to the Global Biobank Engine data. Specifically, this variant has a highly significant association with spleen size in the Bajau population (“Sea Nomads”) in Indonesia⁴². This group has engaged in breath-hold diving for thousands of years and it was found that selection has increased spleen size, providing an oxygen reservoir for diving. Furthermore, we identified 9 variants present in the MEGA array recently associated with COVID-19 infection^{32,33}.

References

1. Groube, L., Chappell, J., Muke, J. & Price, D. A 40,000 year-old human occupation site at Huon Peninsula, Papua New Guinea. *Nature* **324**, 453–455 (1986).
2. Patrick, V. K. *On the road of the winds: an archaeological history of the Pacific Islands before European Contact* (University of California Press, 2017).
3. Sheppard, P., Chiu, S. & Walter, R. Re-dating Lapita Movement into Remote Oceania. *J. Pac. Archaeol.* **6**, 26–36 (2015).
4. Zobel, E. The position of Chamorro and Palauan in the Austronesian family tree: Evidence from verb morphosyntax. In *The history and typology of Western Austronesian voice systems*, 405–434 (The Australian National University, 2002).
5. Jacobs, G. S. *et al.* Multiple Deeply Divergent Denisovan Ancestries in Papuans. *Cell* **177**, 1010–1021.e32 (2019).
6. Larena, M. *et al.* Philippine Ayta possess the highest level of Denisovan ancestry in the world. *Curr. Biol.* **31**, 4219–4230.e10 (2021).
7. Hill, A. V. *et al.* A population genetic survey of the haptoglobin polymorphism in Melanesians by DNA analysis. *Am. J. Hum. Genet.* **38**, 382–9 (1986).
8. O’Shaughnessy, D. F., Hill, A. V. S., Bowdent, D. K., Weatherall, D. J. & Clegg, J. B. Globin Genes in Micronesia: Origins and Affinities of Pacific Island Peoples. *Am. J. Hum. Genet.* **46**, 144–155 (1990).
9. Soares, P. *et al.* Ancient voyaging and Polynesian origins. *Am. J. Hum. Genet.* **88**, 239–247 (2011).
10. Soares, P. A. *et al.* Resolving the ancestry of Austronesian-speaking populations. *Hum. Genet.* **135**, 309–326 (2016).
11. Malaspinas, A. S. *et al.* A genomic history of Aboriginal Australia. *Nature* **538**, 207–214 (2016).
12. Bergström, A. *et al.* A Neolithic expansion, but strong genetic structure, in the independent history of New Guinea. *Science* **357**, 1160–1163 (2017).
13. Choin, J. *et al.* Genomic insights into population history and biological adaptation in Oceania. *Nature* **592**, 583–589 (2021).
14. Alexander, D. H., Novembre, J. & Lange, K. Fast model-based estimation of ancestry in unrelated individuals. *Genome Res.* **19**, 1655–1664 (2009).
15. Ioannidis, A. G. *et al.* Paths and timings of the peopling of Polynesia inferred from genomic networks. *Nature* **597**, 522–526 (2021).
16. Bayman, J. M., Dixon, B. M., Montón-Subías, S. & Segura, N. M. Colonial surveillance, lánchos, and the perpetuation of intangible cultural heritage in guam, mariana islands. *The Glob. Span. Emp.* 222–241 (2020). DOI 10.2307/j.ctv105bb41.14.
17. Callaghan, R. & Fitzpatrick, S. M. On the relative isolation of a micronesian archipelago during the historic period: The palau case-study. *Int. J. Naut. Archaeol.* **36**, 353–364 (2007). DOI 10.1111/j.1095-9270.2007.00147.x.
18. Ioannidis, A. G. *et al.* Native American gene flow into Polynesia predating Easter Island settlement. *Nature* **583**, 572–577 (2020).
19. Pierron, D. *et al.* Genomic landscape of human diversity across madagascar. *Proc. Natl. Acad. Sci.* **114** (2017). DOI 10.1073/pnas.1704906114.
20. Skoglund, P. *et al.* Genomic insights into the peopling of the Southwest Pacific. *Nature* **538**, 510–513 (2016).
21. Lipson, M. *et al.* Population Turnover in Remote Oceania Shortly after Initial Settlement. *Curr. Biol.* **28**, 1157–1165.e7 (2018).

22. Posth, C. *et al.* Language continuity despite population replacement in Remote Oceania. *Nat. Ecol. Evol.* **2**, 731–740 (2018).
23. Hudjashov, G. *et al.* Investigating the origins of eastern Polynesians using genome-wide data from the Leeward Society Isles. *Sci. Reports* **8**, 1823 (2018).
24. Thomson, V. A. *et al.* Using ancient DNA to study the origins and dispersal of ancestral Polynesian chickens across the Pacific. *Proc. Natl. Acad. Sci.* **111**, 4826–4831 (2014).
25. Pugach, I. *et al.* Ancient DNA from Guam and the peopling of the Pacific. *Proc. Natl. Acad. Sci.* **118**, e2022112118 (2021).
26. Patterson, N. *et al.* Ancient Admixture in Human History. *Genetics* **192**, 1065 LP – 1093 (2012).
27. Qin, P. & Stoneking, M. Denisovan Ancestry in East Eurasian and Native American Populations. *Mol. Biol. Evol.* **32**, 2665–2674 (2015).
28. Browning, S. R., Browning, B. L., Zhou, Y., Tucci, S. & Akey, J. M. Analysis of human sequence data reveals two pulses of archaic denisovan admixture. *Cell* **173**, 53–61.e9 (2018).
29. Wang, K., Li, M. & Hakonarson, H. ANNOVAR: functional annotation of genetic variants from high-throughput sequencing data. *Nucleic Acids Res.* **38**, e164–e164 (2010).
30. Landrum, M. J. *et al.* Clinvar: improvements to accessing data. *Nucleic Acids Res* **48**, D835–D844 (2020).
31. SEARCH Collaborative Group, E., Link *et al.* SLCO1B1 variants and statin-induced myopathy—a genomewide study. *N Engl J Med* **359**, 789–799 (2008).
32. COVID-19 Host Genetics Initiative. Mapping the human genetic architecture of COVID-19. *Nature* **600**, 472–477 (2021).
33. Kousathanas, A. *et al.* Whole genome sequencing reveals host factors underlying critical COVID-19. *Nature* (2022).
34. Knapp, S. *et al.* Polymorphisms in interferon-induced genes and the outcome of hepatitis C virus infection: roles of MxA, OAS-1 and PKR. *Genes Immun* **4**, 411–419 (2003).
35. Hamano, E. *et al.* Polymorphisms of interferon-inducible genes OAS-1 and MxA associated with SARS in the Vietnamese population. *Biochem. Biophys Res Commun* **329**, 1234–1239 (2005).
36. Fedetz, M. *et al.* OAS1 gene haplotype confers susceptibility to multiple sclerosis. *Tissue Antigens* **68**, 446–449 (2006).
37. Lim, J. K. *et al.* Genetic Variation in OAS1 Is a Risk Factor for Initial Infection with West Nile Virus in Man. *PLOS Pathog.* **5**, 1–12 (2009).
38. Zeberg, H. & Pääbo, S. A genomic region associated with protection against severe COVID-19 is inherited from Neandertals. *Proc. Natl. Acad. Sci. United States Am.* **118**, 3–7 (2021).
39. Huffman, J. E. *et al.* Multi-ancestry fine mapping implicates OAS1 splicing in risk of severe COVID-19. *Nat. Genet.* **54**, 125–127 (2022).
40. Mendez, F. L., Watkins, J. C. & Hammer, M. F. Global genetic variation at OAS1 provides evidence of archaic admixture in Melanesian populations. *Mol. Biol. Evol.* **29**, 1513–1520 (2012).
41. World Health Organization. Obesity: preventing and managing the global epidemic: report of a WHO consultation (2000).
42. Ilardo, M. A. *et al.* Physiological and Genetic Adaptations to Diving in Sea Nomads. *Cell* **173**, 569–580.e15 (2018).
43. Chang, C.-S. *et al.* A holistic picture of Austronesian migrations revealed by phylogeography of Pacific paper mulberry. *Proc. Natl. Acad. Sci.* **112**, 13537–13542 (2015).

44. Wojcik, G. L. *et al.* Genetic analyses of diverse populations improves discovery for complex traits. *Nature* **570**, 514–518 (2019).
45. Prüfer, K. *et al.* The complete genome sequence of a Neanderthal from the Altai Mountains. *Nature* **505**, 43–49 (2014).
46. Meyer, M. *et al.* A High-Coverage Genome Sequence from an Archaic Denisovan Individual. *Science* **338**, 222–226 (2012).
47. Waterson, R. H., Lander, E. S., Wilson, R. K., Sequencing, T. C. & Consortium, A. Initial sequence of the chimpanzee genome and comparison with the human genome. *Nature* **437**, 69–87 (2005).
48. Behr, A. A., Liu, K. Z., Liu-Fang, G., Nakka, P. & Ramachandran, S. pong: fast analysis and visualization of latent clusters in population genetic data. *Bioinformatics* **32**, 2817–2823 (2016).
49. Delaneau, O., Zagury, J.-F. & Marchini, J. Improved whole-chromosome phasing for disease and population genetic studies. *Nat. Methods* **10**, 5–6 (2013).
50. Maples, B. K., Gravel, S., Kenny, E. E. & Bustamante, C. D. RFMix: A discriminative modeling approach for rapid and robust local-ancestry inference. *The Am. J. Hum. Genet.* **93**, 278 – 288 (2013).
51. Browning, B. L. & Browning, S. R. Improving the accuracy and efficiency of identity-by-descent detection in population data. *Genetics* **194**, 459–471 (2013).
52. Paradis, E. & Schliep, K. ape 5.0: an environment for modern phylogenetics and evolutionary analyses in R. *Bioinformatics* **35**, 526–528 (2019).
53. Moreno-Mayar, J. V. FrAnTK: a Frequency-based Analysis ToolKit for efficient exploration of allele sharing patterns in present-day and ancient genomic datasets. *G3 Genes—Genomes—Genetics* **12** (2021).
54. Minster, R. L. *et al.* A thrifty variant in CREBRF strongly influences body mass index in Samoans. *Nat. Genet.* **48**, 1049–1054 (2016).

Acknowledgements

We thank the participants who contributed samples from the populations included in this study. We recognize the leadership of John Clegg in assembling the collection of materials that enabled the foundation of the Oceanian Genome Variation Project (OGVP). We appreciate the assistance of Michael Alpers, former head of the Papua New Guinea Institute of Medical Research and Professor Sir David John Weatherall (deceased), founder of the Medical Research Council Weatherall Institute of Molecular Biology at the University of Oxford. We thank Euan Ashley and the Oxford-Stanford Big Data Initiative for supporting data generation in partnership with Illumina Inc. We also thank Sarah Kaewert, Chris Gignoux, Gillian Belbin and Eimear Kenny for collaborative input, as well as María Corazón de Ungría and Frederick Delfin for valuable feedback. C.D.Q.C. was supported by a CONACYT Postdoctoral Fellowship and a CINVESTAV visiting professor scholarship. C.B.J., S.V.S., and R.G.B. were supported by CONACYT graduate scholarships. C.D.B. and A.G.I. were supported in part by funds from the Chan Zuckerberg Institute (CZI).

Ethics statement

Individual samples were collected in close collaboration with local partners and institutions by contributing investigators over the last three decades. All samples were collected, following informed consent for genetics studies, storage of genetic material, and use in population genetics research and all have been anonymized. Regulatory approval was obtained from local medical officers as well as health ministry staff from the corresponding state authorities, including the Institute of Medical Research in Papua New Guinea, and approval for this project in particular was provided by the Oxford Tropical Research Ethics Committee (OXTREC) of the University of Oxford (approval reference: OXTREC 537-14).

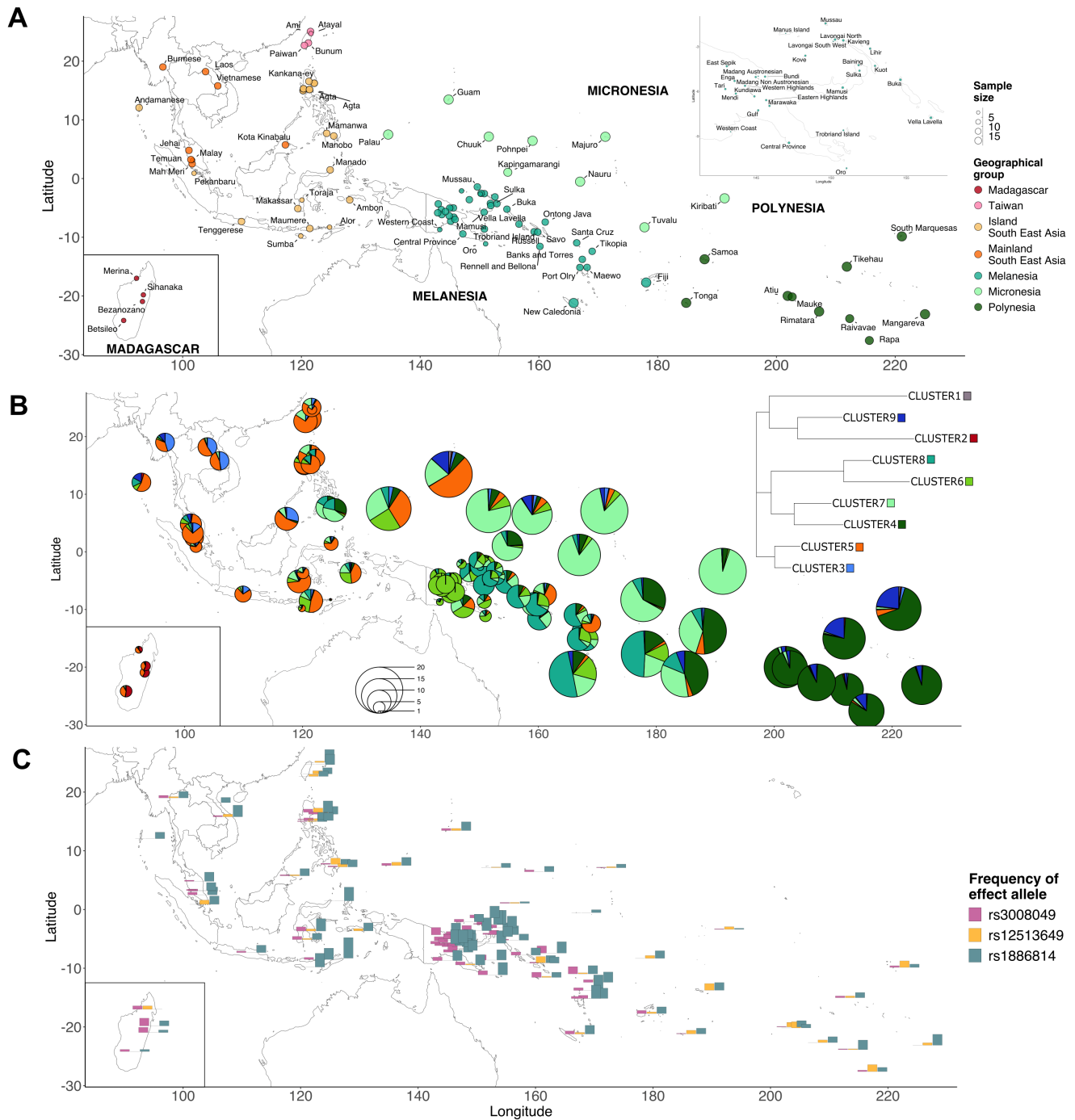


Figure 1. A. Geographic distribution of all the samples used in this study. Each circle represents a population, colored by its geographic location and its size is proportional to the number of samples. **B.** Pie charts show the average ancestry proportions for each location at K=9. The Neighbor-Joining tree shows the relationship between the genetic clusters inferred by ADMIXTURE. **C.** Bar charts show the frequency of 3 variants of clinical interest: rs3008049 - spleen size; rs12513649 - BMI; rs1886814 - COVID.

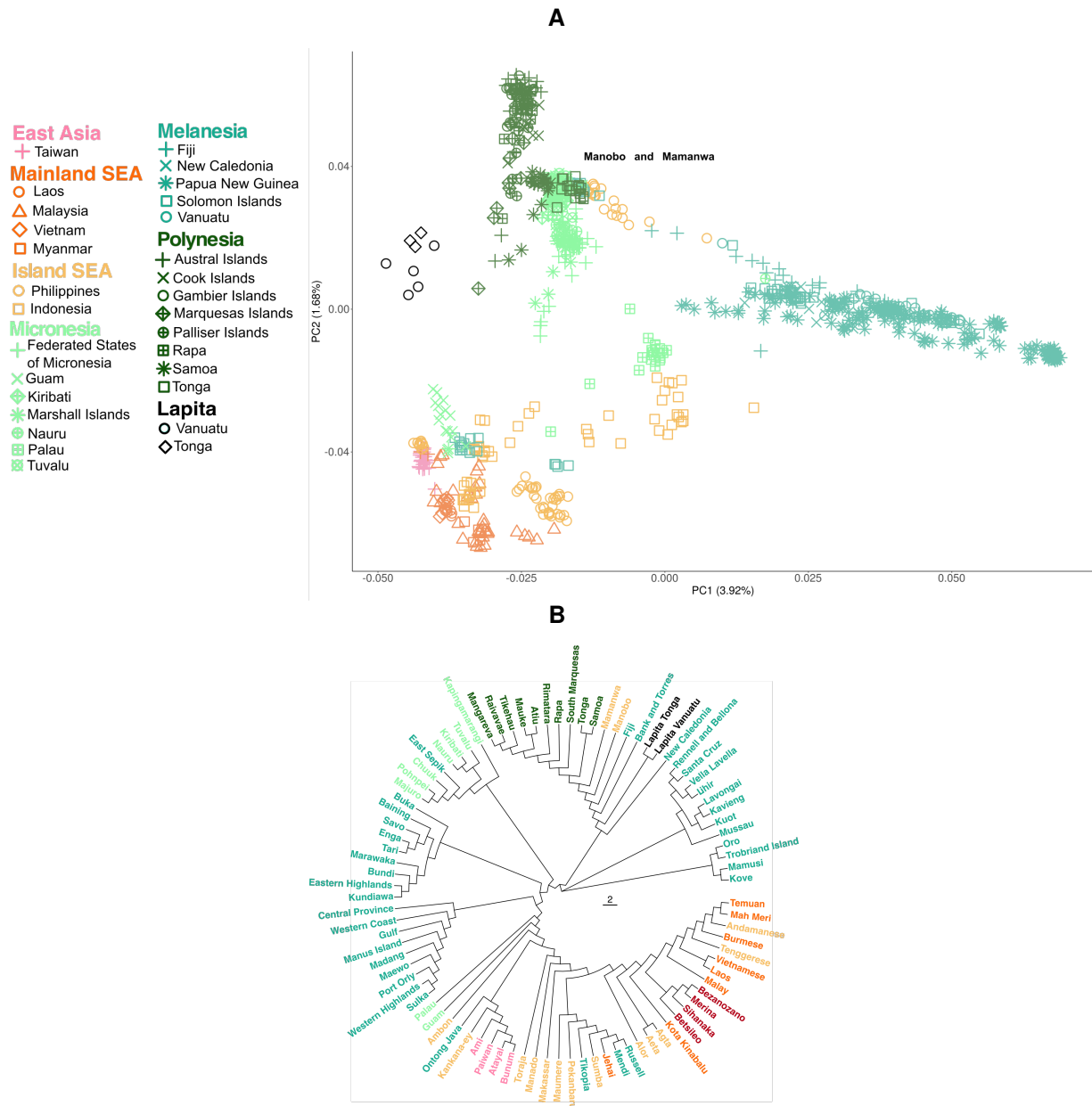


Figure 2. Populations are colored by their geographic group. **A.** Principal component analysis of the OGVP dataset and ancient samples from the Pacific. Ancient Lapita samples are represented as black symbols. **B.** Neighbor-joining tree of the Lapita sequences from Tonga and Vanuatu together with the Austronesian ancestry specific sequences from the modern samples.

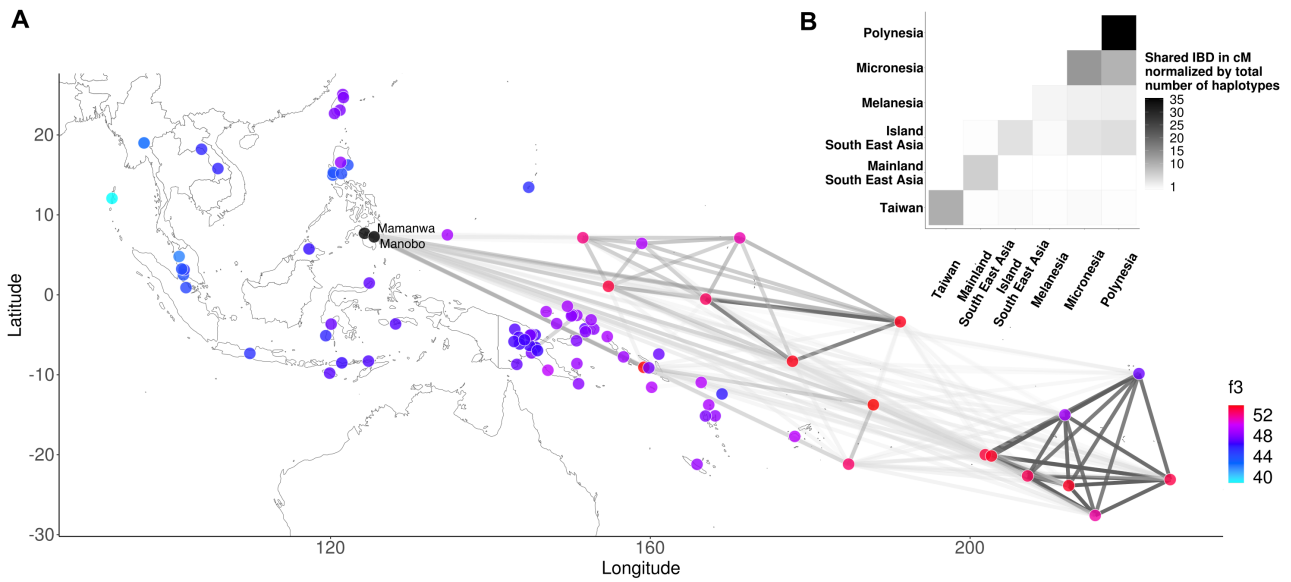


Figure 3. A. Network based on the amount of IBD sharing between populations. The amount of shared IBD is shown as an edge between locations and the color of each edge is relative to the average cM of shared IBD. Only edges with values > 10 cM are shown. The nodes of the network are colored according to the value of the f_3 statistic when Mamanwa and Manobo were used as test populations. **B.** Heatmap representing the amount of shared IBD normalized by the total number of haplotypes in each pair of geographical regions. We do not show Madagascar as it does not share IBD segments with any other populations in the Pacific.

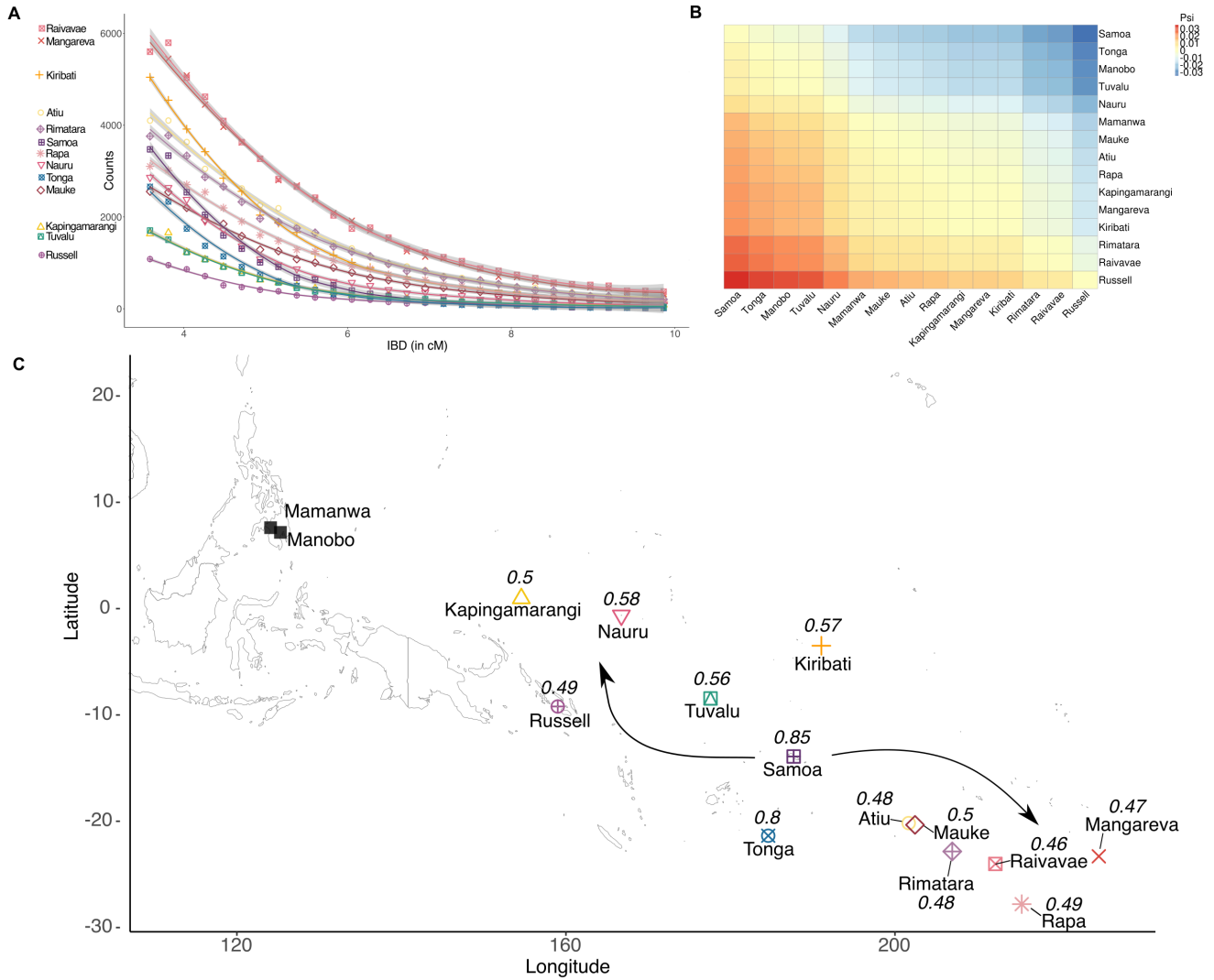


Figure 4. A. IBD segment length distributions for all pairs of individuals in the populations that share ≥ 20 cM with Mamanwa and Manobo, used to fit the exponential decay constants (λ). **B.** Heatmap representing Psi statistic values, it depicts an increase in retained rare variant frequencies along paths of settlements in the Pacific. **C.** Map with the λ results for each of the populations in their geographical location. Symbols in panel A correspond to symbols in panel C. The arrows correspond to the migration directions from Samoa.

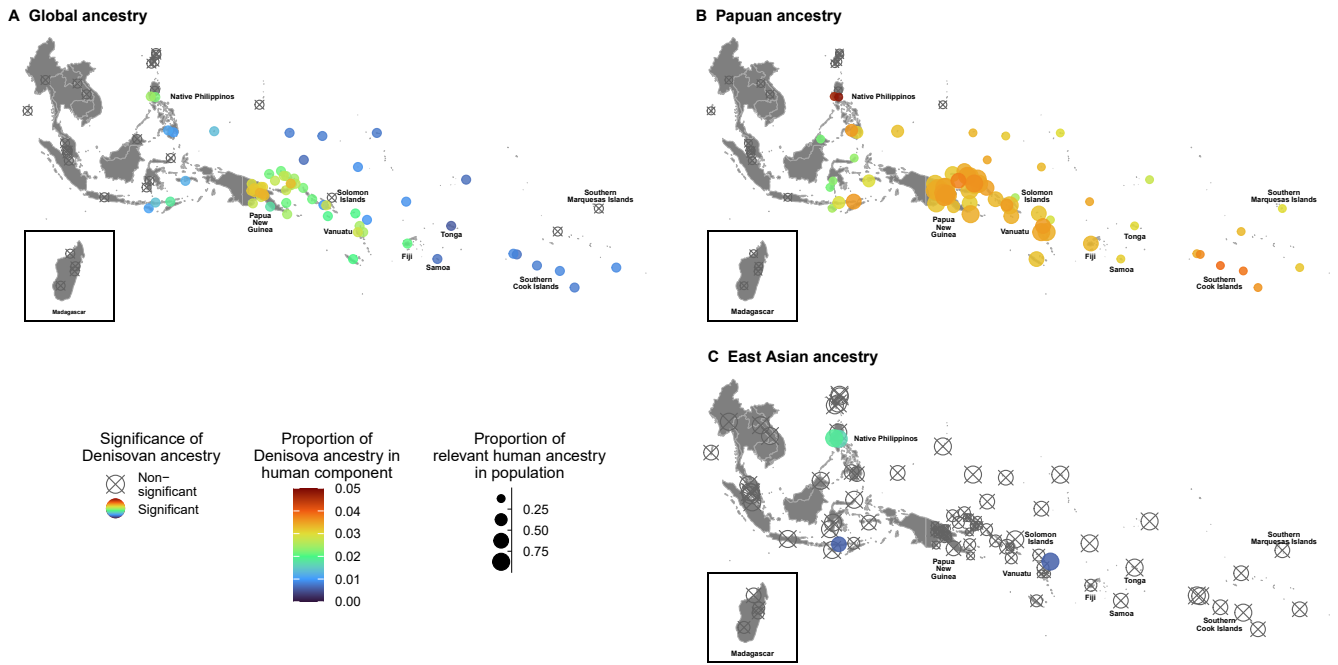


Figure 5. Proportion of Denisovan ancestry estimated by f_4 ratio. A. In global ancestry. B. In Papuan ancestry. C. In East Asian ancestry. Symbol shape distinguishes significant from non-significant Denisovan signal. Symbol color in populations with significant signals give the proportion of Denisovan signals in the ancestry component. Symbol size in panels B and C represents the average proportion of the human ancestry component in each population.

Supplementary material for The Genomic Landscape of Oceania

Consuelo D. Quinto-Cortés^{*1}, Carmina Barberena Jonas^{*1}, Sofía Vieyra-Sánchez^{*1}, Stephen Oppenheimer², Ram González-Buenfil¹, Kathryn Auckland³, Kathryn Robson², Tom Parks², J. Víctor Moreno-Mayar⁴, Javier Blanco-Portillo⁵, Julian R. Homburger⁵, Genevieve L. Wojcik⁶, Alissa L. Severson⁵, Jonathan S. Friedlaender⁷, Francoise Friedlaender⁷, Angela Allen⁸, Stephen Allen^{8,9}, Mark Stoneking^{10,11}, Adrian V. S. Hill², George Aho¹², George Koki¹³, William Pomat¹³, Carlos D. Bustamante⁵, Maude Phipps¹⁴, Alexander J. Mentzer^{2,}, Andrés Moreno-Estrada^{1,**}, and Alexander G. Ioannidis^{15,**}**

****Correspondence: alexander.mentzer@ndm.ox.ac.uk, andres.moreno@cinvestav.mx, ioannidis@ucsc.edu**

May 12, 2024

Supplementary material

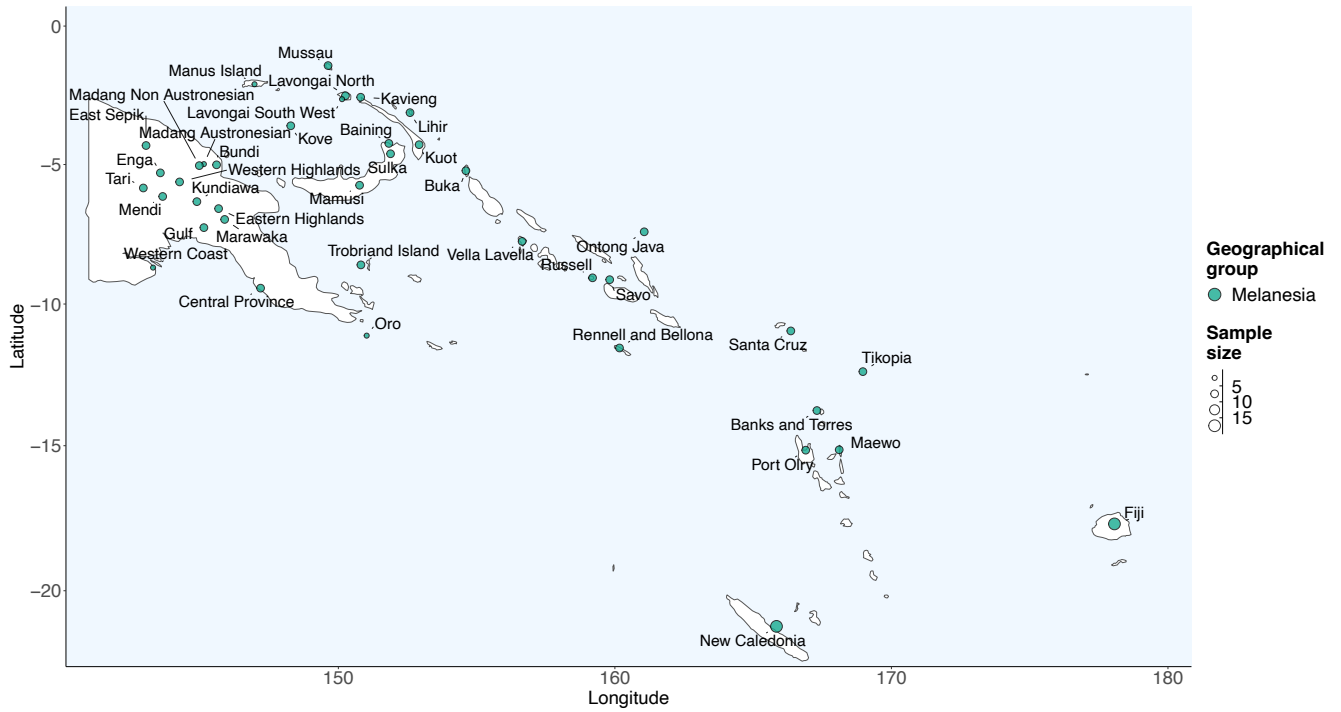
1	Principal component analysis of all the present-day sample data	4
2	ADMIXTURE analysis of the data	5
3	Population pairwise Fst	8
4	Distribution of uniparental lineages	9
4.1	Mitochondrial haplogroups	9
4.2	Chromosome Y haplogroups	11
5	IBD sharing	14
6	f3 statistic	15
7	Denisova introgression	17
8	Clinical relevant variants	20
9	References	26
		26

Supplementary Figures

S1	Geographic distribution of samples in Melanesia	3
S2	Principal component analysis plot of the dataset	4
S3	ADMIXTURE plots from K=2 to K=17	5
S4	ADMIXTURE cross-validation error	6
S5	ADMIXTURE results for K=9 in Melanesia	7
S6	Population pairwise Fst as calculated by smartpca.	8
S7	Geographic distribution of maternal haplogroups	10
S8	Geographical distribution of paternal haplogroups	13
S9	Normalized sum of IBD sharing within OGVP and HGDP continental populations.	14
S10	f3 statistic results	15
S11	IBD sharing between OGVP populations and Manobo and Mananwa	16
S12	Significance of differences of average Denisovan proportion per region	17
S13	D statistic with HGDP and OGVP populations	19
S14	Frequencies of 9 variants associated with COVID-19 infection.	20
S15	Frequencies of 10 variants with a clinical or drug response effect in OGVP.	21

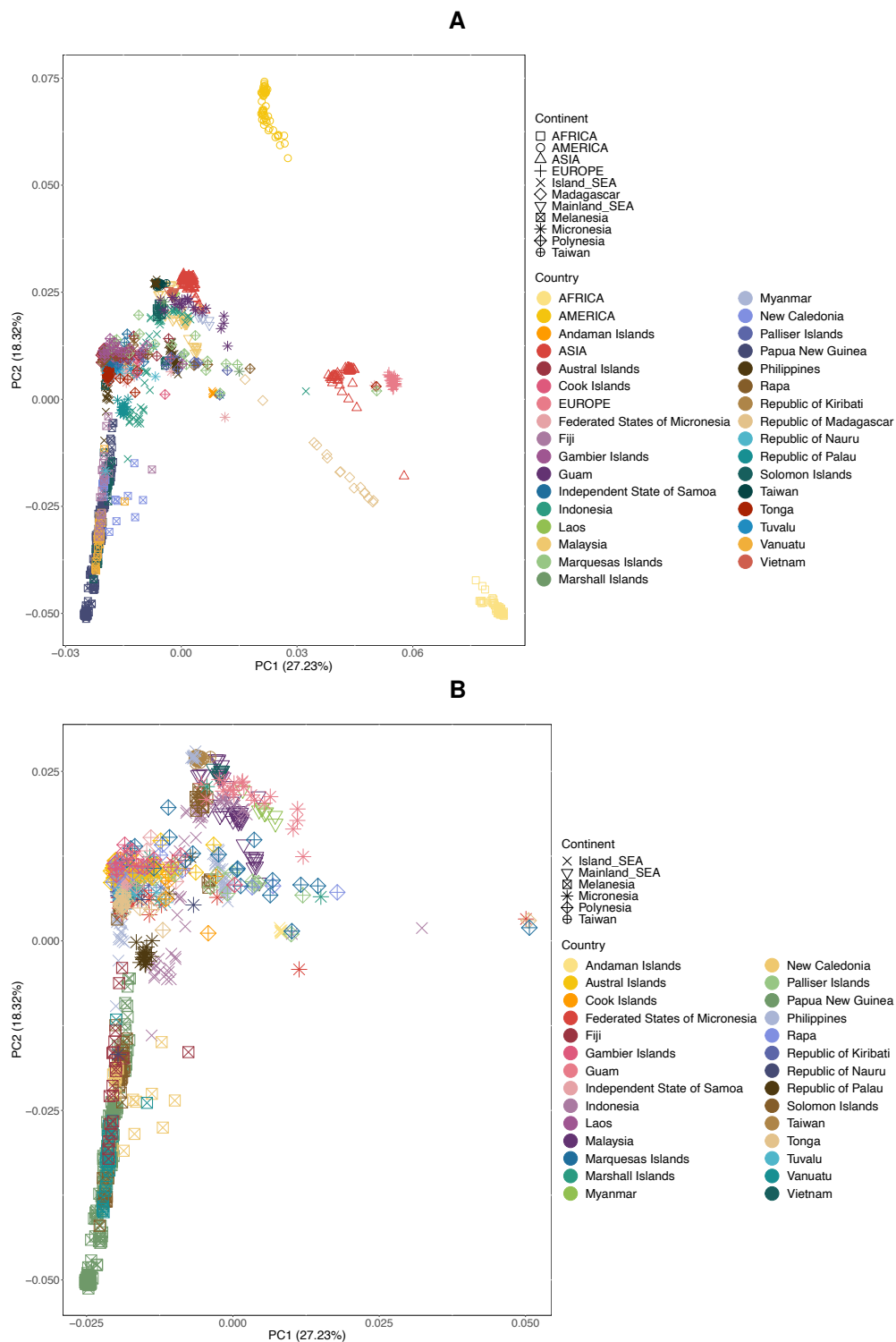
Supplementary Tables

S1	Populations used in this study	22
S2	Ancient and archaic samples used in this study	25



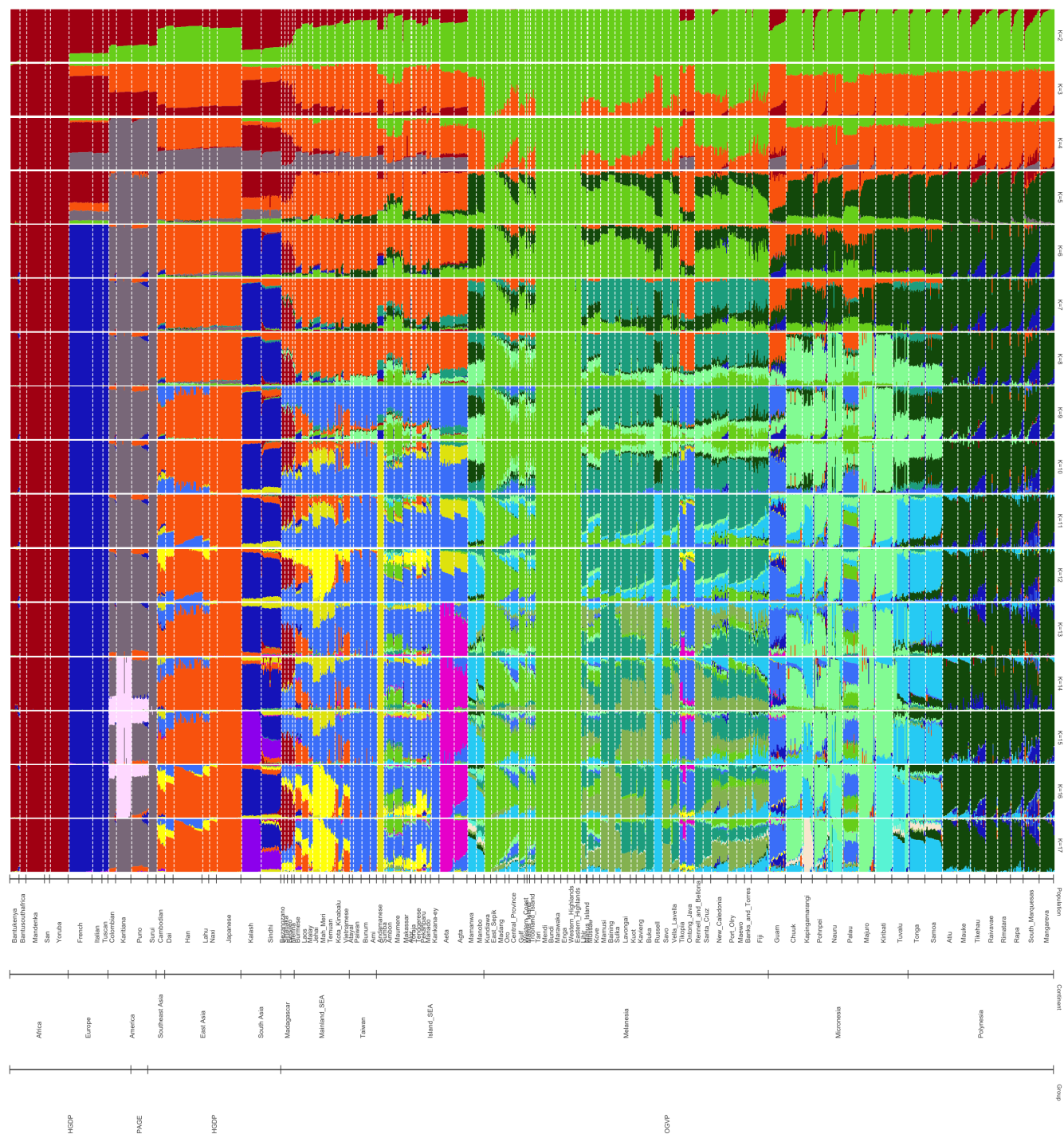
Supplementary Figure S1. Geographical distribution of all the Melanesian samples used in this study. Each circle represents a population, colored by their geographic location and its size is proportional to the number of samples.

1 Principal component analysis of all the present-day sample data



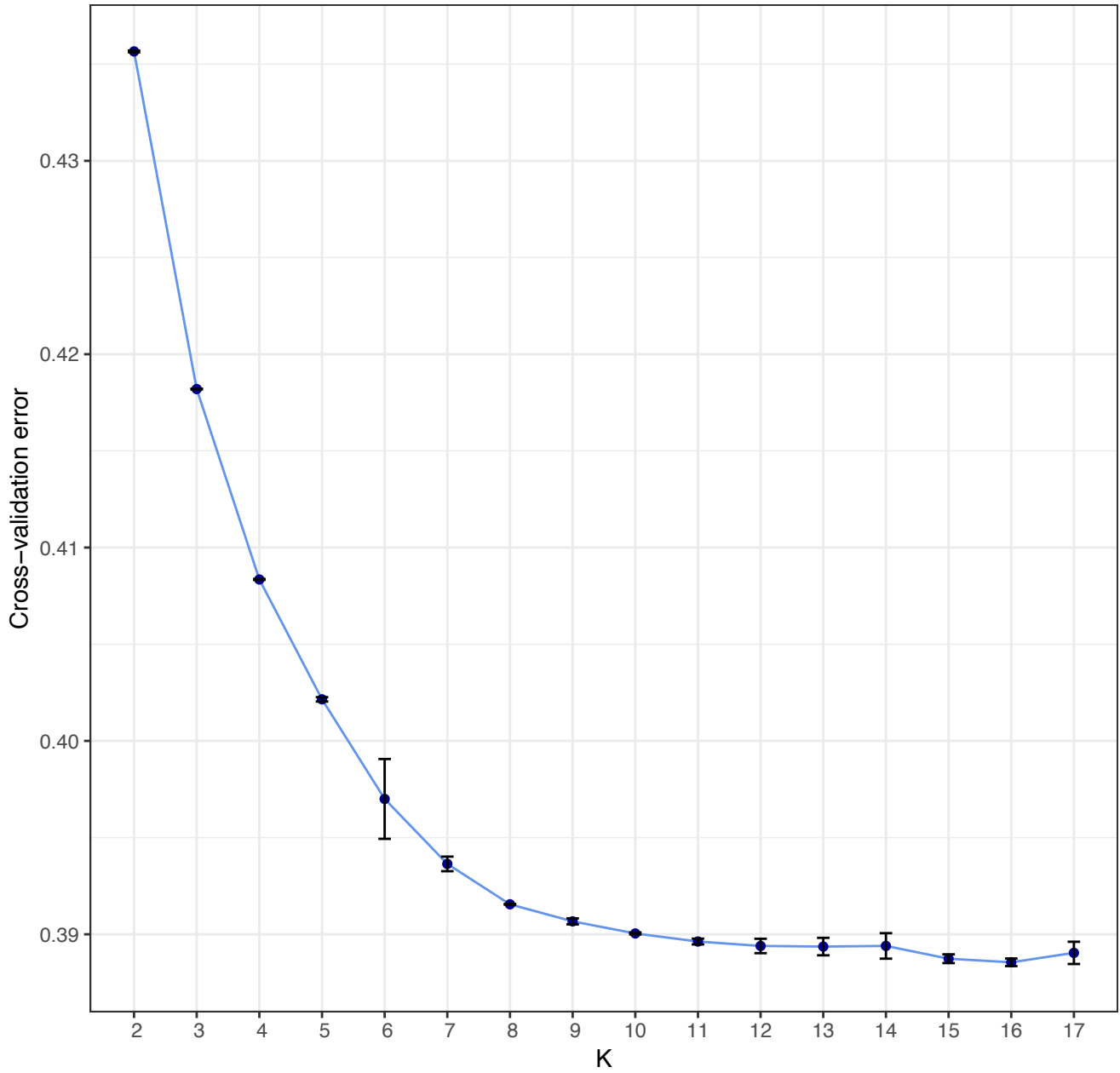
Supplementary Figure S2. A. Principal component analysis plot of all samples together with selected HGDP populations. These continental reference populations are written in capital letters. **B.** Principal component analysis plot of only the samples in this study. removed Madagascar has been removed from both figures for clarity.

2 ADMIXTURE analysis of the data

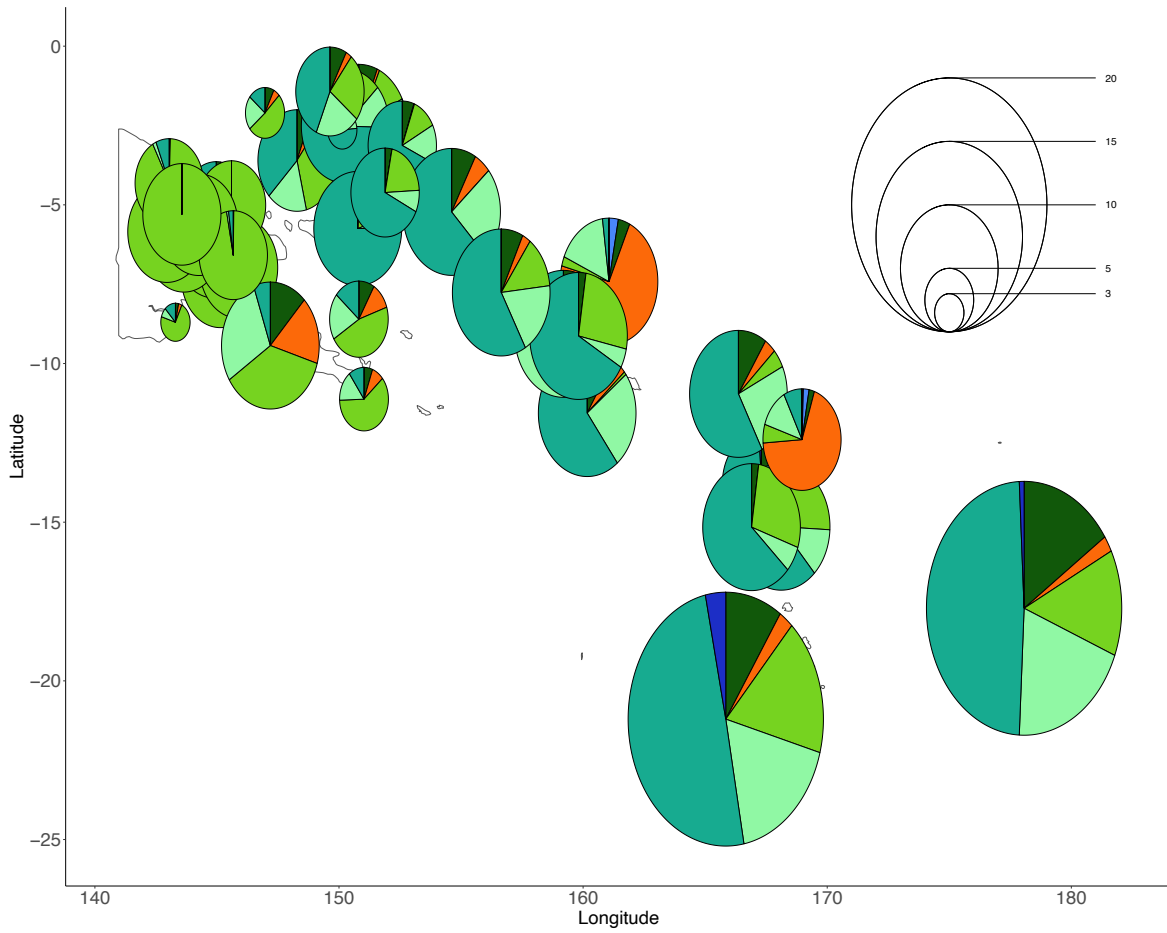


Supplementary Figure S3. ADMIXTURE plots from K=2 to K=17. Genetic clustering was done with ADMIXTURE¹ and we show the representative mode for each K as identified with pong².

Cross-validation error for ADMIXTURE runs K2-17

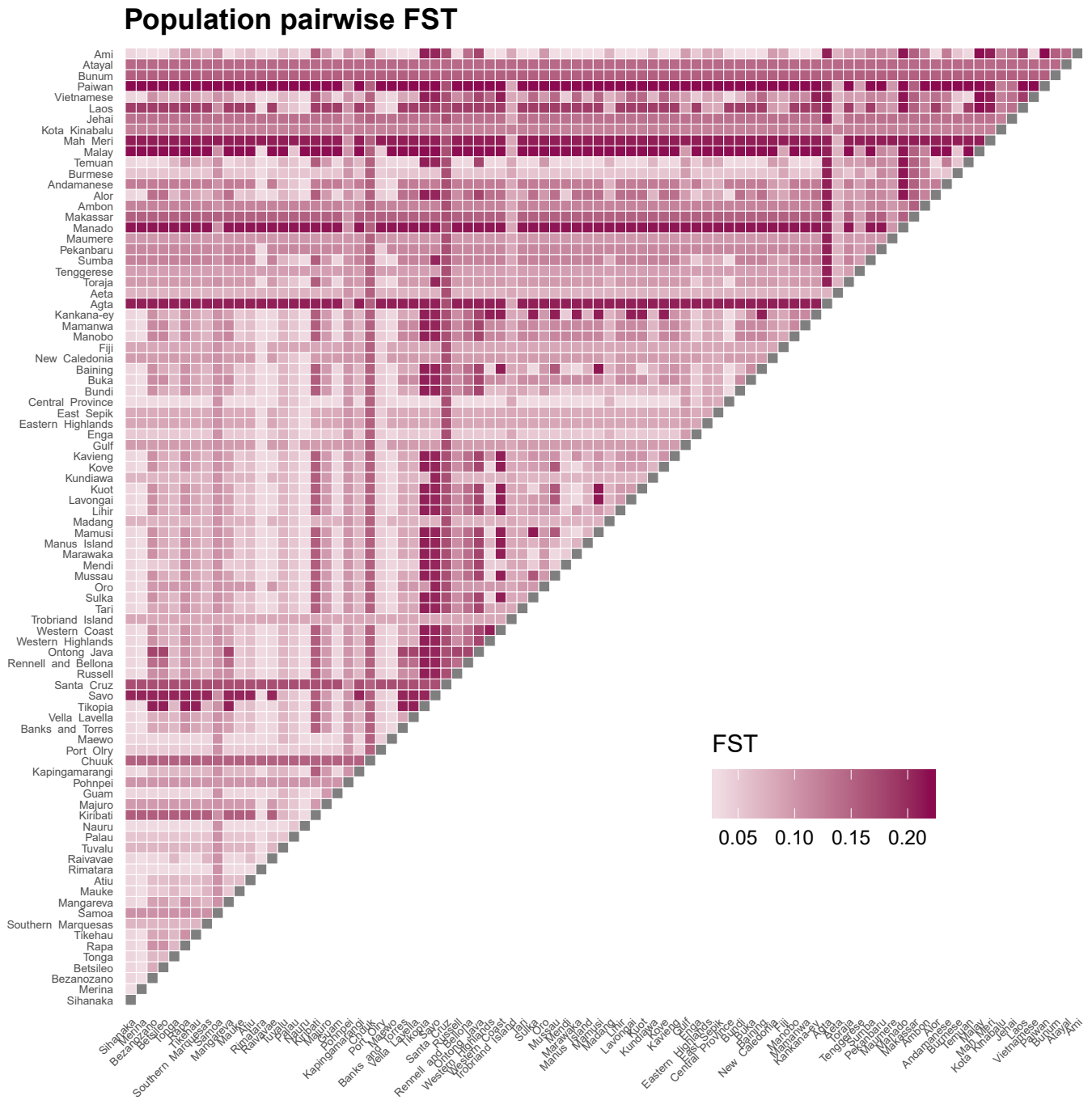


Supplementary Figure S4. Cross-validation errors of 10 replicates of ADMIXTURE for each K. The point represents the mean and the whiskers the standard deviation of each of the replicates.



Supplementary Figure S5. ADMIXTURE results for K=9 in Melanesia. Each pie chart corresponds to a population. The size of each pie-chart is proportional to the population's sample size. Pie-chart slices represent the proportions of each group in the population.

3 Population pairwise Fst



Supplementary Figure S6. Population pairwise Fst as calculated by `smartpca`. Darker colors represent higher Fst values.

4 Distribution of uniparental lineages

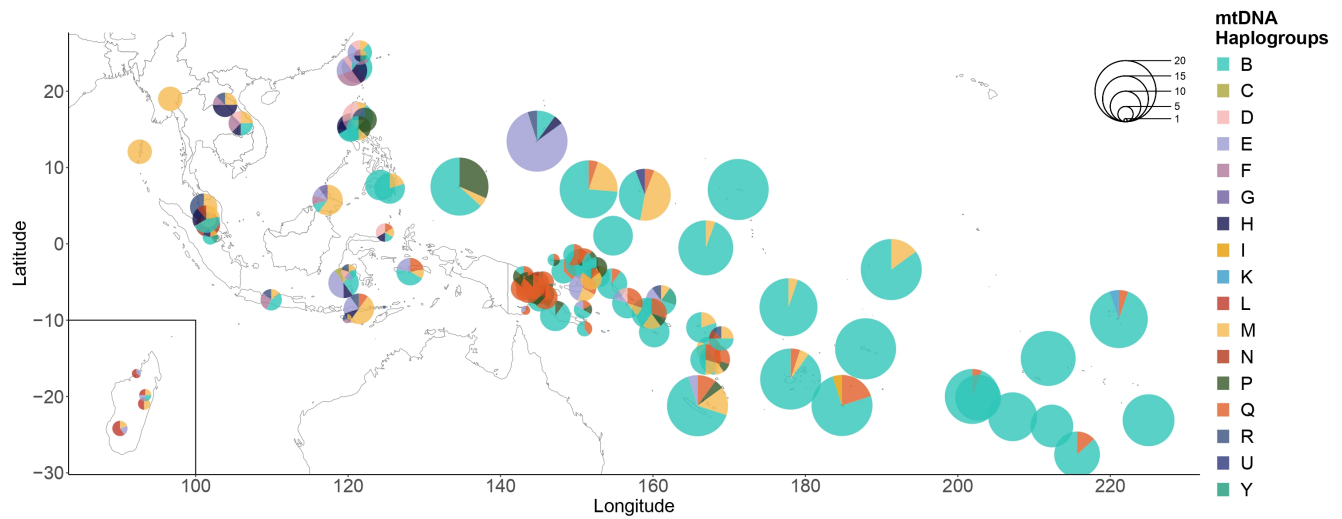
We used the program Haplogrep2³ to examine the diversity of mitochondrial haplogroups, and we utilized Snappy⁴ to look at the variety of chromosome Y lineages. We use the nomenclature of the International Society of Genetic Genealogy. Y-DNA Haplogroup Tree 2019-2020, Version: 15.73.

4.1 Mitochondrial haplogroups

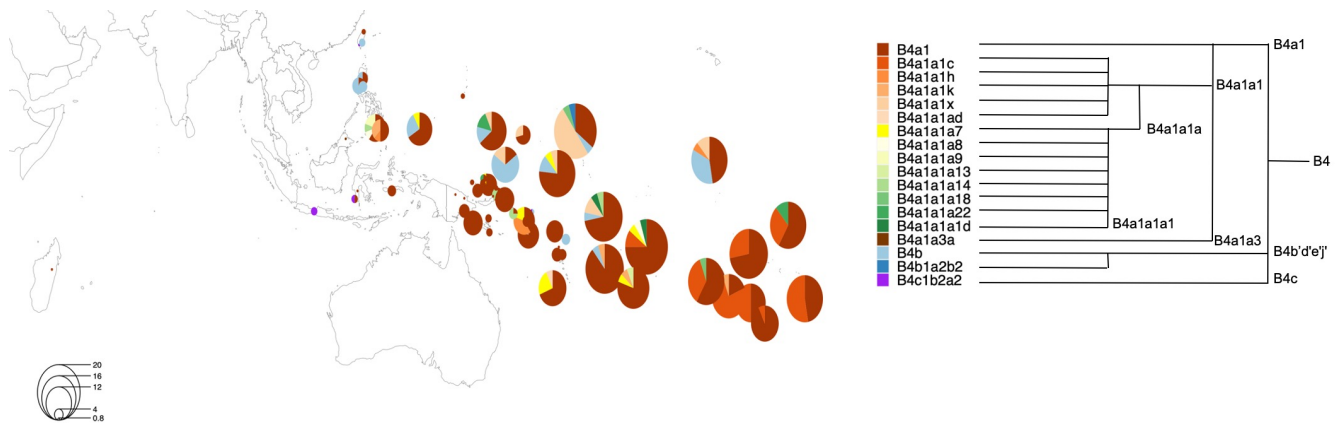
The most common haplogroup seen in the Pacific is haplogroup B4, in particular haplogroup B4a1 and its derivatives (Figures S7A and S7B). Among them, we can find the so-called “Polynesian motif” that defines a mitochondrial lineage that is only present in Austronesian-speaking populations and almost reaches fixation in Polynesia. This motif originated more than 6000 years ago near the Bismarck Archipelago and its immediate ancestor is practically restricted to Near Oceania, and has been seen in previous studies⁵.

We also observe the haplogroup Q in the Highlands and other populations of Papua New Guinea. Haplogroup P is also very frequent in the Eastern Highlands and in the Agta population from the Philippines. We observe a few occurrences of the maternal haplogroup M7c (that derives ultimately out of Taiwan around 3,000 to 4,000 years ago⁶) in samples from Island Southeast Asia, in Pohnpei, Tuvalu, Chuuk, Kiribati, Nauru, Tikopia, Ontong Java and in one Bezanozano individual from Madagascar.

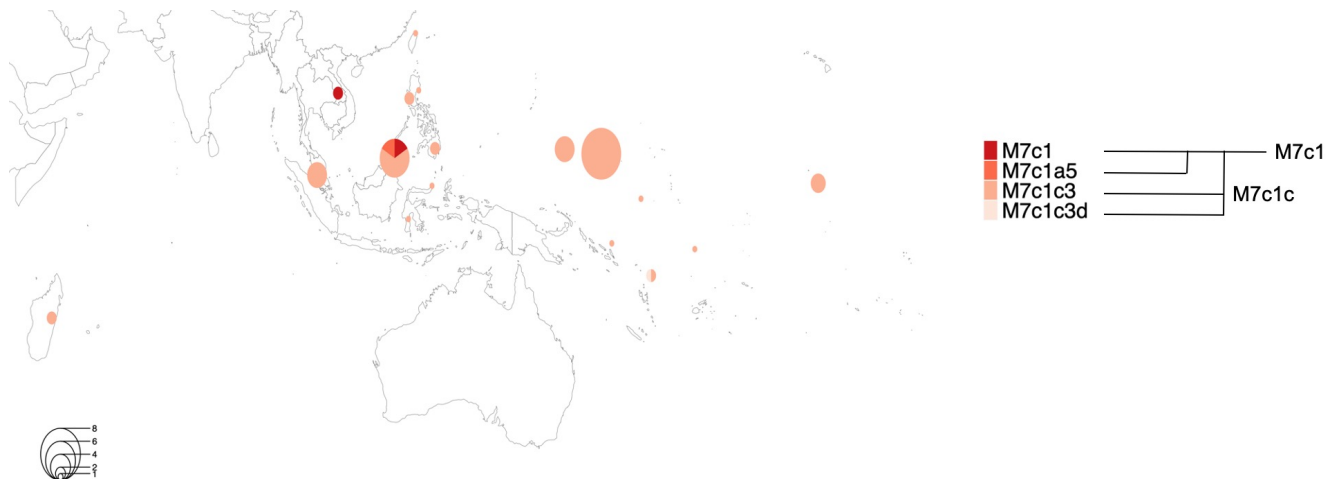
Haplogroup E is found in Guam, Madagascar, the Bismarck Archipelago, Ontong Java and Taiwan. The presence of this haplogroup in Oceania might be explained by migrations from Mainland South East Asia via Island South East Asia^{6,7}. Other haplogroups found in this dataset are H, F, R, L, and Y, K, G, U, C, I, N in small percentages.



A



B



C

Supplementary Figure S7. A. Distribution of the maternal haplogroups in all of the populations in this study. B. Distribution of mtDNA haplogroup B4. C. Distribution of mtDNA haplogroups M7c. Circle radius is proportional to sample size and the colors in the pie chart and tree aim to reflect the relationship between the haplogroups.

4.2 Chromosome Y haplogroups

In contrast, we find a greater variety of parental haplogroups and different patterns in Melanesia (haplogroups S and M), Micronesia (K and O) and Polynesia (C, R and Q) (Figure S8). Consistent with the ADMIXTURE results in Polynesia, the European and Native American influences are evident from the presence of R and Q haplogroups.

Haplogroup C is thought to be one of the original haplogroups present in Oceania, explaining its ubiquity in the region⁸. Consistent with previous findings, we observe C1a2a (V182) localized to Southeast Asia and derived subclades C1b2a (M38) and C1b2a1 (M208) are restricted to Papuan New Guinea, Melanesia, Micronesia, and Polynesia^{9,10}. It has been proposed that this divide suggests the derived haplogroups originated in Melanesia⁹. Interestingly, we also observe haplogroup C1b2a1 in Manobo and Mananwa individuals. In Polynesia, C1b2a1 is by far the most abundant haplogroup on all islands. This suggests that either the settling populations were largely C1b2a1, or this haplogroup has replaced the haplogroup of the settling populations.

Like C, haplogroup K is also thought to be one of the founding haplogroups in Oceania, which leads to its prevalence throughout the region⁹. Our findings are consistent with previous works⁹⁻¹¹. Specifically, K2b1 (P397/399) exists at low frequencies in Indonesia and Malaysia, high frequencies amongst Filipino native groups, and throughout Oceania, with high frequencies in Micronesia^{9,11}.

Haplogroup S is thought to have originated in New Guinea and spread outward^{9,10}. In accordance with this, it is most common and concentrated in New Guinea and in some individuals from Micronesia. We observe haplogroup S1a1b (M320) in Melanesia as well as Indonesia and in one Y chromosome in Guam. Lineage S1a2a (P307) is found across Melanesia and Micronesia.

Haplogroup M is a subgroup of K, and has previously been observed and low to moderate frequencies in Indonesia and Malaysia, and high frequencies in Papua New Guinea and Melanesia⁹⁻¹¹. M (SK1828/S322) is most concentrated in Papua New Guinea. M1 (M5) is found in one individual from Alor, one individual from Tonga and in a number of Highlanders from Papua New Guinea. M1a1a2a (P87) is found in coastal Papua New Guinea. M2 (M353) is restricted to Melanesia.

Haplogroup P (P295) has previously been reported in Aeta populations in the Philippines¹¹. Consistent with this, we find it in those populations as well as in two samples from Manado.

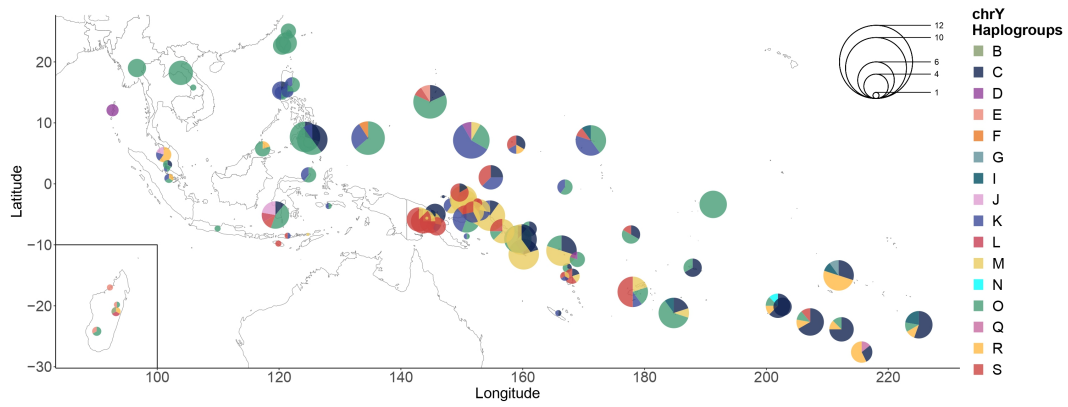
Haplogroup O probably originated in East Asia and later migrated into the South Pacific. The lineage expanded into Taiwan (high frequency in the aboriginal Taiwanese), Indonesia, Melanesia, Micronesia, and Polynesia. We see a high diversity of lineages of this haplogroup in our dataset. Haplogroups O1a1 (M119) and O1a1a (M307.1) are common in the Philippines, Melanesia and Micronesia. In Taiwan, these lineages achieve high frequency in Taiwan, and are thought to mark the Austronesian expansion and spread of agricultural technology^{9,10}. Derivatives of O1b1 are found in Mainland Southeast Asia, Melanesia and Madagascar. In particular, haplogroup O1a2 (M110) has been shown to link Oceania to Taiwan¹⁰.

Haplogroup O2 (F36) is thought to have originated in Southeast Asia and later spread through Oceania, with O2a2 (P201) marking the expansion of agriculture⁹. Derivatives of O2a2b can be found in Mainland and Island Southeast Asia, Micronesia and Polynesia.

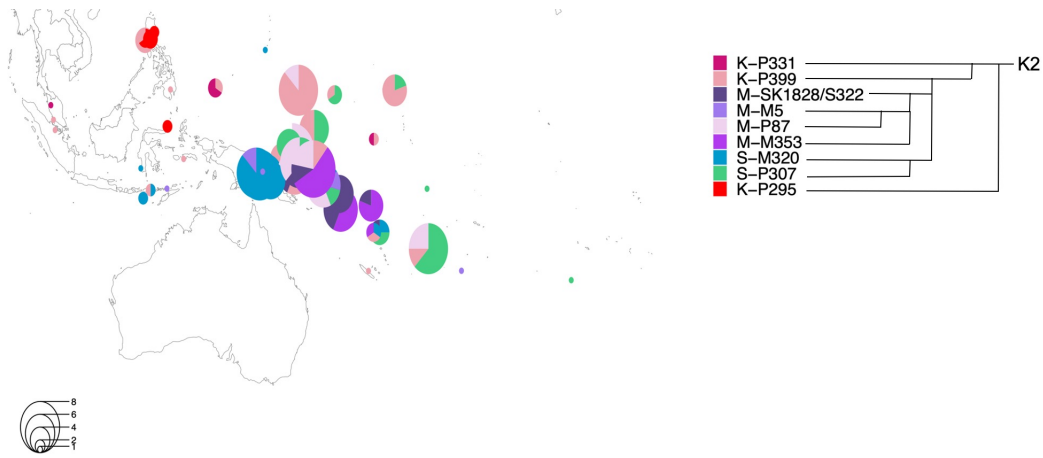
Throughout Indonesia and Malaysia we find the presence of haplogroups common in the Middle East and South Asia, which may be due to the history of trade with Muslim merchants, and the presence of Islam in the region. Two R2a haplogroups are present in Malaysia and Indonesia. Three J2a1(L27) haplogroups are present in Makassar and Jehai Negrito, however J2 may also have a European origin. A haplogroup L1a1 (M27) is present in Makassar, Indonesia and L1a2 (M357) in the Bezanozono people in Madagascar. We also find haplogroups more commonly found in Asia. We observe one N (M231) in Atiu. One F (M89/PF2746) is present in Palau. All 4 males in the Andaman Islands are D1a (CTS11577), which matches previous findings¹². D1a2a1c1a~D-CTS1670/Z1546 is found in Chuuk (Micronesia), which is notable because D1a2a (M64.1/M55) is a Japanese group, so this may be a consequence of Japanese occupation during World War II.

Haplogroups of European ancestry (I1a, I2, R1, G2) are present throughout Oceania, Micronesia, and Indonesia, reflecting recent exploration and colonization. The R1a and R1b haplogroups are the most common and widespread, followed by I and G2b1 (M377) in Tikehau. As expected, we found 6 African Y chromosomes, almost entirely in populations from Madagascar: One B2a1a1a1 (M109) is present in the Bezanozono and E1b1a1a1a2a1 (M4254)

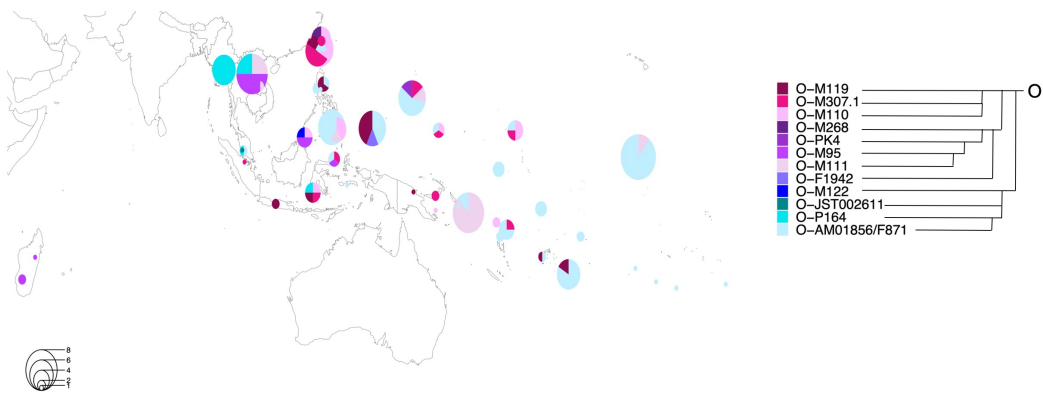
Y chromosomes in the Sihanaka, Betsileo, and Merina populations. One E1b1a1a1a2a1 (M4254) haplogroup is present in Guam, which is likely the consequence of recent admixture. Finally, we find one Q1b1a1a (M3) in Rapa Iti and is likely a consequence of the Peruvian slave trade.



A



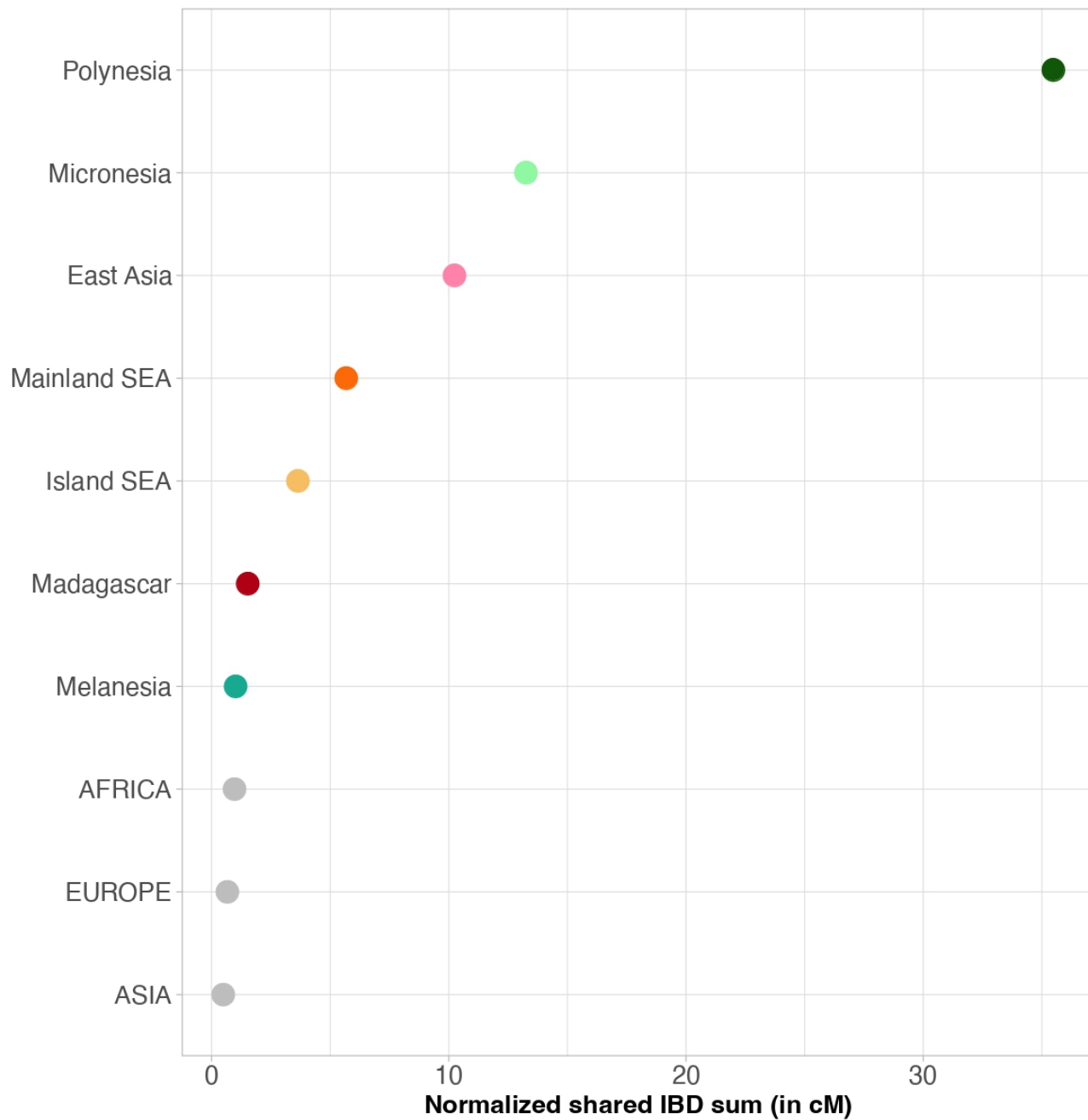
B



C

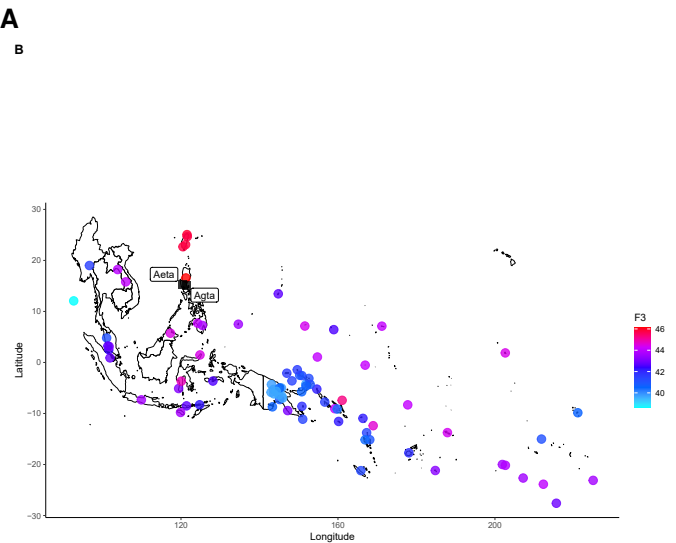
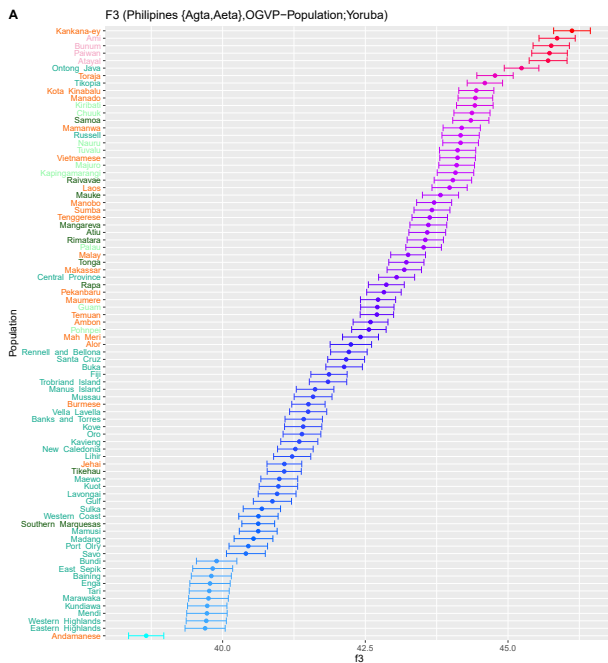
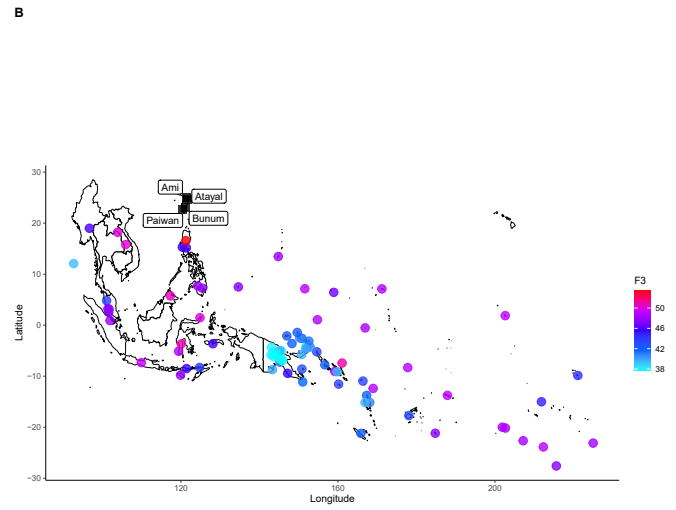
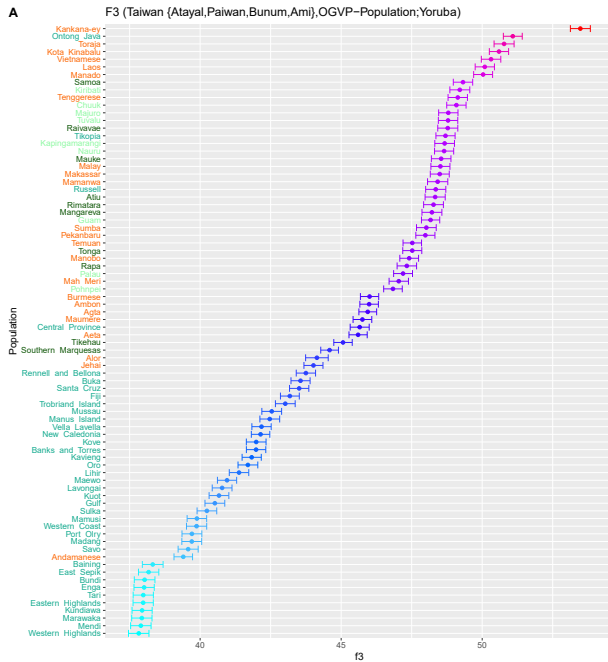
Supplementary Figure S8. **A.** Distribution of all the paternal haplogroups in the study. **B.** Distribution of chrY haplogroups K. **C.** Distribution of chrY haplogroups O. Circle radius is proportional to sample size and the colors in the pie chart and tree try to reflect the relationship between the haplogroups. We use the mutation name of the haplogroups instead of their common names.

5 IBD sharing

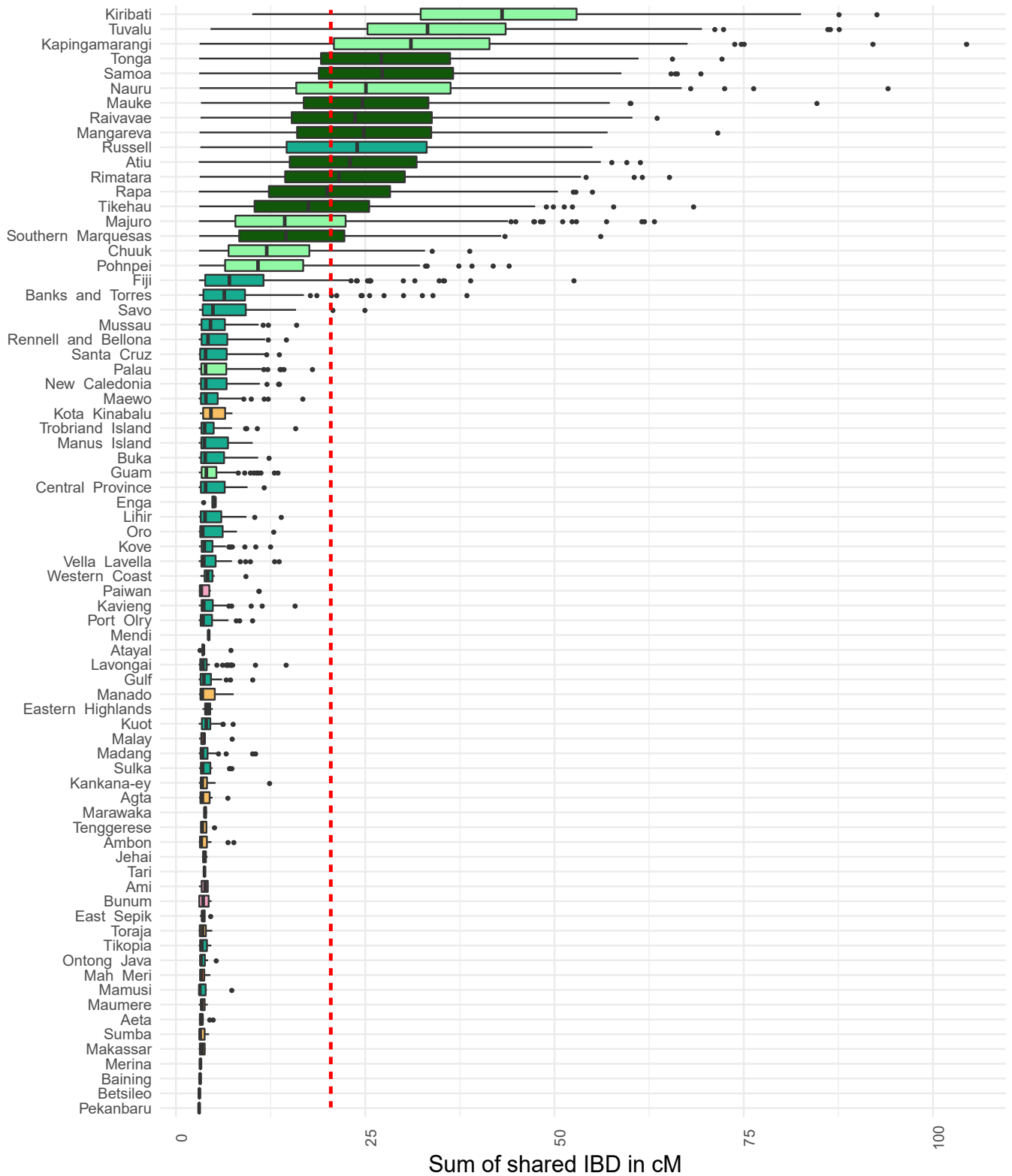


Supplementary Figure S9. Normalized sum of IBD sharing within OGVP and HGDP continental populations. Gray points with uppercase labels represent continental references. Other points represent OGVP regions, and the color for each of the region is the same as those in Figure 1A.

6 f3 statistic

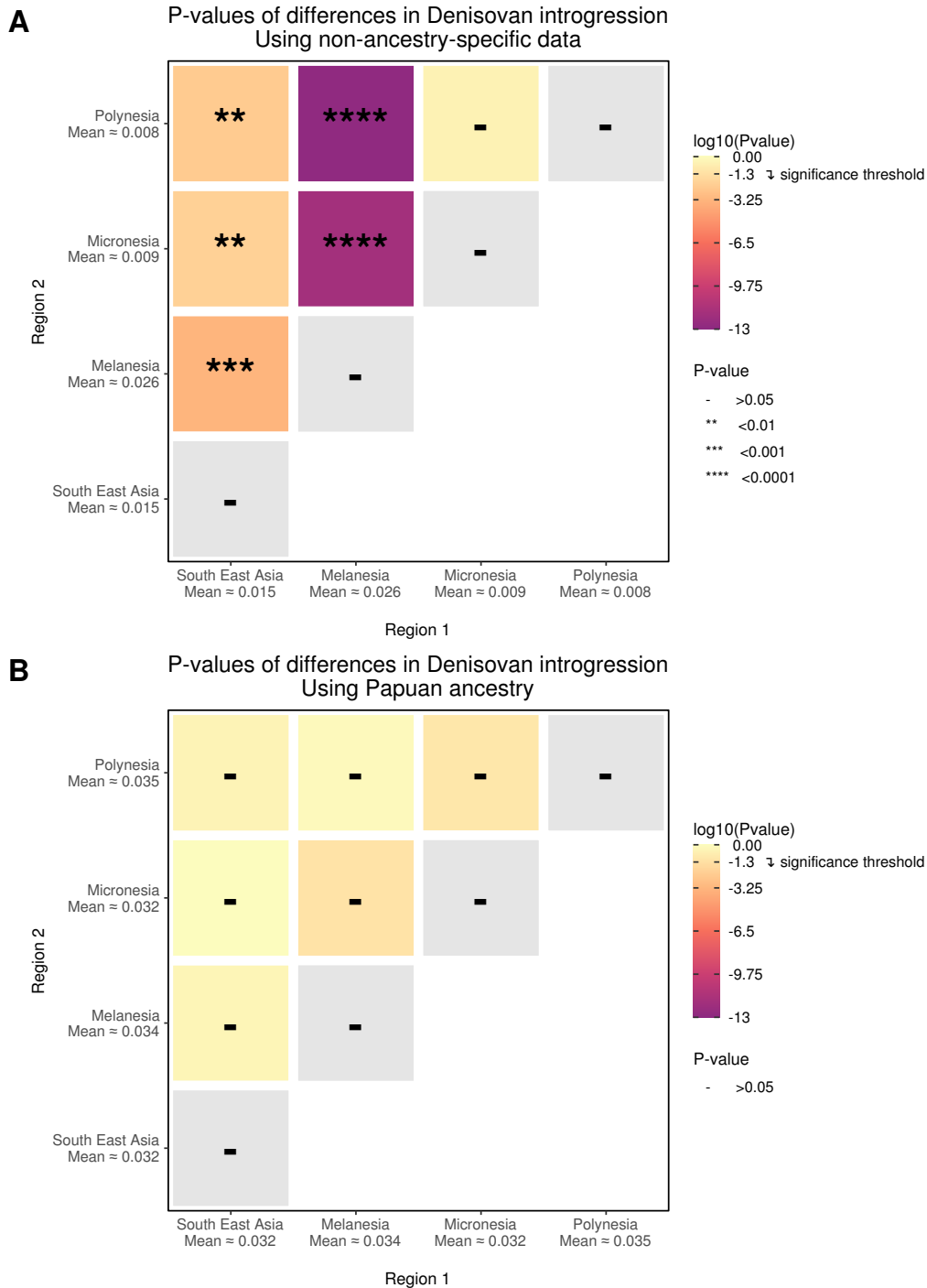


Supplementary Figure S10. Results of the f_3 statistic test with **A.** Taiwan and **B.** Northern Philippines (Agta and Aeta) as test populations. For each panel, both plots offer complementary visualizations of the same data. Population labels in left-hand plots are colored by region using the same colors used in Figure 1A.



Supplementary Figure S11. Boxplots representing IBD sharing between OGVP populations and Manobo and Mananwa. We established a cut-off of 20cM of shared IBD to investigate further the relationship between these populations, shown as a dotted red line. Box plots are colored by region using the same colors used in Figure 1A.

7 Denisova introgression



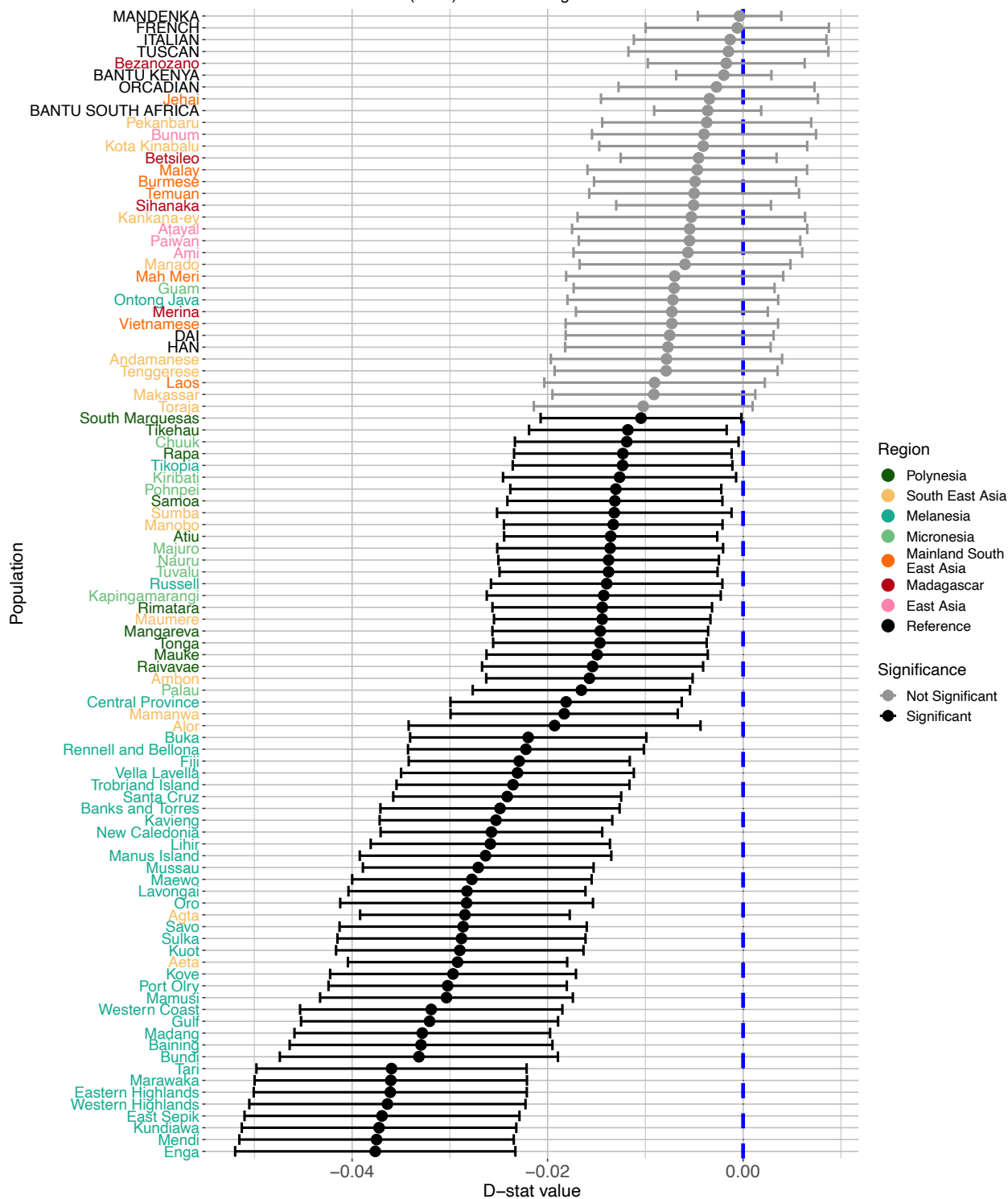
Supplementary Figure S12. Significance of differences of average Denisovan proportion per region using **A.** global ancestry data and **B.** Papuan ancestry data. Darker colors represent lower $\log_{10}(\text{p-values})$. Symbols in the heatmap represent ranges of p-values.

To confirm our results using the D statistic to test for the presence of Denisova introgression in OGVP, we also included reference populations from HGDP¹³ (Figure S13). We included populations from Africa, Europe and continental Asia in which case the D statistic should be zero or closer to this value. This is in agreement with our results. All the D statistic values for these populations are close to zero and are not significant. This observation gives us more confidence in the application of this method to our data.

D-stat values. Test: D(Yoruba, X; Denisova, Chimpanzee)

Average SNPs used per population: 61959.

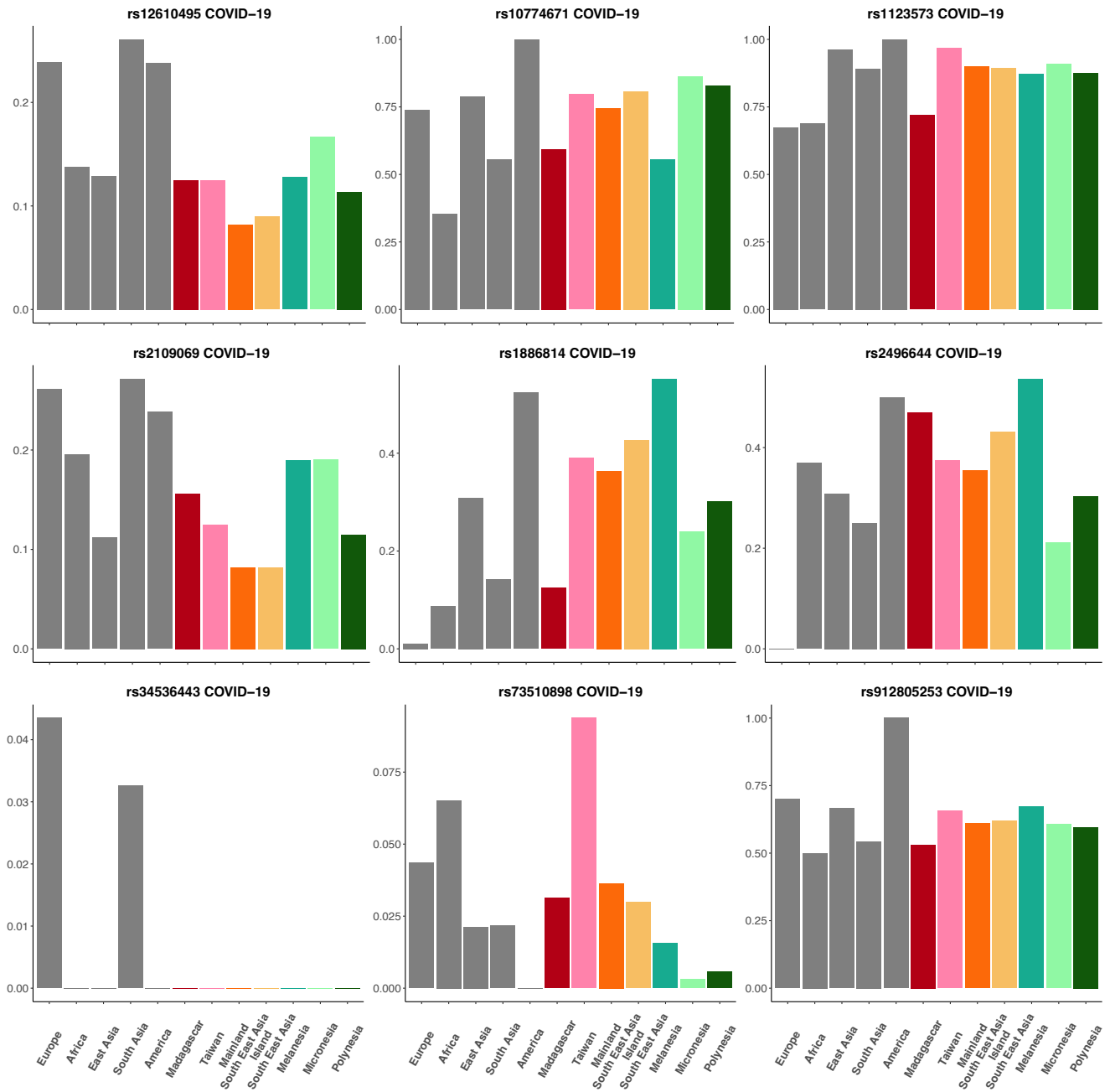
Confidence intervals are $D \pm (3 * SE)$. Values are significant if Z-score is > 3 or < -3 .



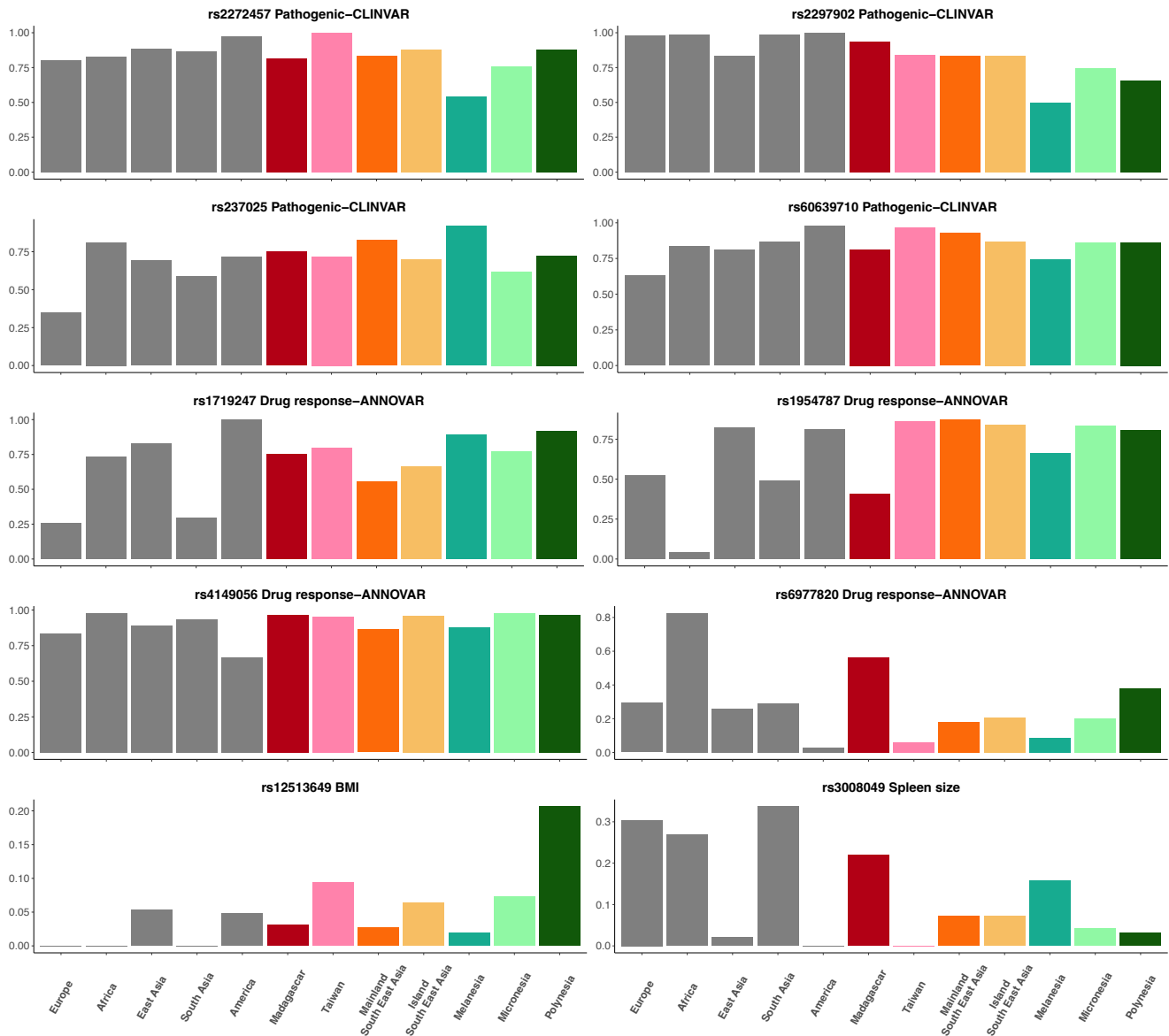
Supplementary Figure S13. D statistic with OGVP populations and continental references from HGDP.

Continental references are labeled in black capital letters. OGVP population labels are colored by region using the same colors used in Figure 1A.

8 Clinical relevant variants



Supplementary Figure S14. Frequencies of 9 variants associated with COVID-19 infection. Bars for continental references are shown in gray. Bars for OGVP data are colored by region using the same colors used in Figure 1A.



Supplementary Figure S15. Frequencies of 10 variants with a clinical or drug response effect in OGVP. Bars for continental references are shown in gray. Bars for OGVP data are colored by region using the same colors used in Figure 1A.

Supplementary Table S1. Populations used in this study

Population	Location	Region	Country	Group	Latitude	Longitude	Sample Size
Betsileo	Madagascar	Madagascar	Republic of Madagascar	Madagascar	-22.18115	45.066509	5
Bezanozano	Madagascar	Madagascar	Republic of Madagascar	Madagascar	-18.9465859	48.2301345	4
Merina	Madagascar	Madagascar	Republic of Madagascar	Madagascar	-14.9901932	47.2340012	3
Sihanaka	Madagascar	Madagascar	Republic of Madagascar	Madagascar	-17.8199064	48.3834	4
Ami	-	East Asia	Taiwan	East Asia	25.05553546	121.5302419	8
Atayal	-	East Asia	Taiwan	East Asia	24.680534	121.607299	4
Bunun	-	East Asia	Taiwan	East Asia	23.0978451	121.1754608	10
Paiwan	-	East Asia	Taiwan	East Asia	22.679355	120.499213	10
Burmese	-	Mainland South East Asia	Myanmar	Mainland South East Asia	18.999818	96.67104	8
Laos	-	Mainland South East Asia	Laos	Mainland South East Asia	18.209382	103.859154	8
Vietnamese	-	Mainland South East Asia	Vietnam	Mainland South East Asia	15.793925	105.910208	8
Jehai	-	Mainland South East Asia	Malaysia	Mainland South East Asia	4.801136	101.056993	9
Kota Kinabalu, Sabah, Malaysia	Kota Kinabalu, Sabah, Malaysia	Mainland South East Asia	Malaysia	Mainland South East Asia	5.739969	117.304542	10
Mah Meri	-	Mainland South East Asia	Malaysia	Mainland South East Asia	2.5	101.5980053	8
Malay	-	Mainland South East Asia	Malaysia	Mainland South East Asia	3.138506	101.686989	5
Ternuan	-	Mainland South East Asia	Malaysia	Mainland South East Asia	3.232223	101.380967	9
Andamanese	Andaman Islands	Island South East Asia	Andaman Islands	Island South East Asia	12.070593	92.661495	8
Aeta	Aglao, Zambales, Luzon	Island South East Asia	Philippines	Island South East Asia	14.976736	120.28102	8
Aeta	Sta Juliana, Tarlac, Luzon	Island South East Asia	Philippines	Island South East Asia	15.299905	120.348187	9
Aeta	Cozo, Aurora, Luzon	Island South East Asia	Philippines	Island South East Asia	16.238306	122.163252	8
Aeta	Umtirey, Aurora, Luzon	Island South East Asia	Philippines	Island South East Asia	15.164057	121.36559	8
Kankana-ey (Austronesian)	Luzon	Island South East Asia	Philippines	Island South East Asia	16.56623	121.26263	10
Mamanwa	Mindanao	Island South East Asia	Philippines	Island South East Asia	7.696724	124.252279	10
Manobo	Mindanao	Island South East Asia	Philippines	Island South East Asia	7.253365	125.451072	10
Alor	Alor	Island South East Asia	Indonesia	Island South East Asia	-8.291119	124.740476	1
Ambon	Ambon	Island South East Asia	Indonesia	Island South East Asia	-3.642288	128.137297	9
Makassar	South Sulawesi	Island South East Asia	Indonesia	Island South East Asia	-5.111489	119.402628	10
Manado	North Sulawesi	Island South East Asia	Indonesia	Island South East Asia	1.4748305	124.8420794	6
Maumere	Flores	Island South East Asia	Indonesia	Island South East Asia	-8.509977	121.40829	10
Pekanbaru	Riau, Sumatra	Island South East Asia	Indonesia	Island South East Asia	0.898428	101.919073	5
Sumba	Sumba	Island South East Asia	Indonesia	Island South East Asia	-9.796582	119.88713	3
Tenggerese	Java	Island South East Asia	Indonesia	Island South East Asia	-7.328187	109.90769	7
Toraja	South Sulawesi	Island South East Asia	Indonesia	Island South East Asia	-3.66358	120.078157	5
Baining	New Britain, Bismarck Archipelago	Bismarck Archipelago	Papua New Guinea	Melanesia	-4.2393857	151.826541	8
Kove	Bismarck Archipelago	Bismarck Archipelago	Papua New Guinea	Melanesia	-3.6032459	148.2789778	8

Table S1 continued from previous page

Population	Location	Region	Country	Group	Latitude	Longitude	Sample Size
Lavongai	North, Bismarck Archipelago, New Ireland Province	Bismarck Archipelago	Papua New Guinea	Melanesia	-2.5164284	150.257396	9
Lavongai	South-West, Bismarck Archipelago, New Ireland Province	Bismarck Archipelago	Papua New Guinea	Melanesia	-2.5164284	150.257396	3
Mamusi	New Britain, Bismarck Archipelago	Bismarck Archipelago	Papua New Guinea	Melanesia	-5.7465904	150.7679216	9
Mamus Island	Manus Province, Bismarck Archipelago	Bismarck Archipelago	Papua New Guinea	Melanesia	-2.102639	146.968728	4
Mussau	Mussau Island, St. Matthias Islands, Bismarck Archipelago	Bismarck Archipelago	Papua New Guinea	Melanesia	-1.428844	149.628553	7
Sulka	New Britain, Bismarck Archipelago	Bismarck Archipelago	Papua New Guinea	Melanesia	-4.6128943	151.8877321	7
Central Province	-	Coastal Papua New Guinea and Northern Islands	Papua New Guinea	Melanesia	-9.4336552	147.1877643	10
East Sepik (Non Austronesian)	East Sepik Province	Coastal Papua New Guinea and Northern Islands	Papua New Guinea	Melanesia	-4.3150058	143.045893	7
Gulf (Non Austronesian)	-	Coastal Papua New Guinea and Northern Islands	Papua New Guinea	Melanesia	-7.2691821	145.1375834	8
Madang (Non Austronesian)	Madang Province	Coastal Papua New Guinea and Northern Islands	Papua New Guinea	Melanesia	-4.98497	145.13758	7
Madang (Austronesian)	Madang Province	Coastal Papua New Guinea and Northern Islands	Papua New Guinea	Melanesia	-4.98497	145.13758	3
Oro	Oro Province	Coastal Papua New Guinea and Northern Islands	Papua New Guinea	Melanesia	-11.123267	151.024229	5
Trobriand Island	Milne Bay Province	Coastal Papua New Guinea and Northern Islands	Papua New Guinea	Melanesia	-8.602934	150.815458	6
Western Coast	-	Coastal Papua New Guinea and Northern Islands	Papua New Guinea	Melanesia	-8.7	143.3	3
Fiji	-	Melanesia	Fiji	Melanesia	-17.71337	178.06503	20
Ontong Java	Malaita Province	Melanesia	Solomon Islands	Melanesia	-7.418758	161.060837	10
Rennell and Bellona	Province of Solomon Islands	Melanesia	Solomon Islands	Melanesia	-11.361522	160.166898	10
Russell	Russell Islands, Central Province	Melanesia	Solomon Islands	Melanesia	-9.065272	159.192378	10
Santa Cruz	Santa Cruz Islands, Temotu Province	Melanesia	Solomon Islands	Melanesia	-10.956548	166.362137	10
Savo	Savo Island, Central Province	Melanesia	Solomon Islands	Melanesia	-9.131841	159.812064	10
Tikopia	Temotu Province	Melanesia	Solomon Islands	Melanesia	-12.398055	168.968108	8
Vella Lavella	Western Province	Melanesia	Solomon Islands	Melanesia	-7.761974	156.64547	10
New Caledonia	New Caledonia	New Caledonia	New Caledonia	Melanesia	-21.206088	165.844116	20
Bundi	South Madang Province, Eastern Highlands	Papua New Guinea Highlands	Papua New Guinea	Melanesia	-5.011016	145.596128	7
Eastern Highlands	Eastern Highlands	Papua New Guinea Highlands	Papua New Guinea	Melanesia	-6.5861674	145.6689636	7
Enga	Highlands	Papua New Guinea Highlands	Papua New Guinea	Melanesia	-5.3005849	143.5635637	8
Kundiawa	Chimbu Province	Papua New Guinea Highlands	Papua New Guinea	Melanesia	-6.335598	144.884146	8
Marawaka	Eastern Highlands	Papua New Guinea Highlands	Papua New Guinea	Melanesia	-6.9743628	145.8885379	8
Mendi	Central Southern Highlands	Papua New Guinea Highlands	Papua New Guinea	Melanesia	-6.1493907	143.6474817	8
Tari	Southern Highlands	Papua New Guinea Highlands	Papua New Guinea	Melanesia	-5.84472	142.94722	8
Western Highlands	Western Highlands	Papua New Guinea Highlands	Papua New Guinea	Melanesia	-5.6268128	144.2593118	8

Table S1 continued from previous page

Population	Location	Region	Country	Group	Latitude	Longitude	Sample Size
Kaviang	New Ireland Province	Papua New Guinea New Ireland Province	Papua New Guinea	Melanesia	-2.572532	150.807159	10
Kuot	New Ireland Province	Papua New Guinea New Ireland Province	Papua New Guinea	Melanesia	-4.2853256	152.9205918	7
Lihir	Lihir Island, Bismarck Archipelago	Papua New Guinea New Ireland Province	Papua New Guinea	Melanesia	-3.129295	152.5922298	7
Buka	Buka Island, Bougainville Region	Solomon Islands	Papua New Guinea	Melanesia	-5.222642	154.612741	10
Banks and Torres	Banks Islands and Torres Islands, Torba, Vanuatu	Vanuatu	Vanuatu	Melanesia	-13.768686	167.305904	8
Maewo	Maewo Island, Penama Province, Vanuatu	Vanuatu	Vanuatu	Melanesia	-15.142532	168.111849	10
Port Olry	Espiritu Santo, Vanuatu	Vanuatu	Vanuatu	Melanesia	-15.156158	166.900709	10
Chuuk	Chuuk State, Federated States of Micronesia	Federated States of Micronesia	Federated States of Micronesia	Micronesia	7.138676	151.559307	19
Kapingamarangi	Pohnpei State, Federated States of Micronesia	Federated States of Micronesia	Federated States of Micronesia	Micronesia	1.065879	154.759943	13
Pohnpei	Pohnpei State, Federated States of Micronesia	Federated States of Micronesia	Federated States of Micronesia	Micronesia	6.432848	158.933281	17
Guam	Guam	Micronesia	Guam	Micronesia	13.450812	144.788818	20
Kiribati	Republic of Kiribati	Micronesia	Republic of Kiribati	Micronesia	-3.370417	-168.734039	20
Majuro	Marshall Islands	Micronesia	Marshall Islands	Micronesia	7.1164214	171.1857736	20
Nauru	Republic of Nauru	Micronesia	Republic of Nauru	Micronesia	-0.52798	166.935153	18
Palau	Republic of Palau	Republic of Palau	Republic of Palau	Micronesia	7.5	134.616667	19
Tuvalu	Tuvalu	Tuvalu	Tuvalu	Micronesia	-8.309632	177.780762	19
Aitiu	Southern Islands of the Cook Islands	Cook Islands	Cook Islands	Polynesia	-19.9965795	-158.1069946	18
Mauke	Cook Islands	Cook Islands	Cook Islands	Polynesia	-20.16063	-157.33841	15
Mangareva	Gambier Islands, French Polynesia	French Polynesia	Gambier Islands	Polynesia	-23.10965	-134.97434	17
Rarvavae	Austral Islands, French Polynesia	French Polynesia	Austral Islands	Polynesia	-23.86498	-147.6609	14
Rapa	Bass Islands, French Polynesia	French Polynesia	Rapa	Polynesia	-27.5924	-144.35218	15
Rimatara	Austral Islands, French Polynesia	French Polynesia	Austral Islands	Polynesia	-22.65269	-152.80882	16
South Marquesas	Marquesas Islands	French Polynesia	Marquesas Islands	Polynesia	-9.8582413	-138.8799972	19
Tikehau	Palliser Islands Tuamotu Archipelago, French Polynesia	French Polynesia	Palliser Islands	Polynesia	-15.01578	-148.14373	18
Samoa	Independent State of Samoa	Polynesia	Independent State of Samoa	Polynesia	-13.751823	187.896161	20
Tonga	Kingdom of Tonga	Polynesia	Tonga	Polynesia	-21.178986	-175.198242	20

Supplementary Table S2. Ancient and archaic samples used in this study

Sample	Location	Country	Group	Mean Date BP (dates)	Latitude	Longitude	Reference(s)
I1368	Efate Island, Vanuatu, Teouma Lapita site	Vanuatu	Melanesia	2870 (2990-2740)	-17.574499913492648	168.41432199165033	14
I1369	Efate Island, Vanuatu, Teouma Lapita site	Vanuatu	Melanesia	2885 (3000-2750)	-17.574499913492648	168.41432199165033	14
I1370	Efate Island, Vanuatu, Teouma Lapita site	Vanuatu	Melanesia	2945 (3110-2780)	-17.574499913492648	168.41432199165033	14
MAL006	Malakula	Vanuatu	Melanesia	2495 (2690-2320)	-16.073881	167.447786	15
TON001	Tongatapu	Tonga	Polynesia	2475 (2670-2320)	-21.177119	-175.109078	15
TON002	Tongatapu	Tonga	Polynesia	2475 (2690-2350)	-21.177119	-175.109078	15
CP30	Talasiu Site, Fanga 'Uta Lagoon	Tonga	Polynesia	2510 (2680-2340)	-21.14518581979385	-175.2044433513414	14
Altai Neanderthal	Denisova Cave, Altai Mountains	Russia	Asia	50,300 ± 2,200 years	51.409	84.689	16
Altai Denisova	Denisova Cave, Altai Mountains	Russia	Asia	74,000 - 82,000 years	51.409	84.689	17
Chimpanzee	-	-	-	-	-	-	18

9 References

1. Alexander, D. H., Novembre, J. & Lange, K. Fast model-based estimation of ancestry in unrelated individuals. *Genome Res.* **19**, 1655–1664 (2009).
2. Behr, A. A., Liu, K. Z., Liu-Fang, G., Nakka, P. & Ramachandran, S. pong: fast analysis and visualization of latent clusters in population genetic data. *Bioinformatics* **32**, 2817–2823 (2016).
3. Weissensteiner, H. *et al.* Haplogrep 2: mitochondrial haplogroup classification in the era of high-throughput sequencing. *Nucleic Acids Res.* **44**, W58–W63 (2016).
4. Severson, A. L. *et al.* SNAPPY: Single Nucleotide Assignment of Phylogenetic Parameters on the Y chromosome. *bioRxiv* (2018).
5. Soares, P. *et al.* Ancient voyaging and Polynesian origins. *Am. J. Hum. Genet.* **88**, 239–247 (2011).
6. Soares, P. A. *et al.* Resolving the ancestry of Austronesian-speaking populations. *Hum. Genet.* **135**, 309–326 (2016).
7. Brandão, A. *et al.* Quantifying the legacy of the Chinese Neolithic on the maternal genetic heritage of Taiwan and Island Southeast Asia. *Hum. Genet.* **135**, 363–376 (2016).
8. Bergström, A. *et al.* Deep roots for aboriginal australian y chromosomes. *Curr Biol* **26** (2016).
9. Karafet, T. M. *et al.* Major East–West Division Underlies Y Chromosome Stratification across Indonesia. *Mol. Biol. Evol.* **27**, 1833–1844 (2010).
10. Kayser, M. The Human Genetic History of Oceania: Near and Remote Views of Dispersal. *Curr. Biol.* **20**, R194–R201 (2010).
11. Karafet, T. M., Mendez, F. L., Sudoyo, H., Lansing, J. S. & Hammer, M. F. Improved phylogenetic resolution and rapid diversification of Y-chromosome haplogroup K-M526 in Southeast Asia. *Eur. J. Hum. Genet.* **23**, 369–373 (2015).
12. Mondal, M. *et al.* Y-Chromosomal sequences of diverse indian populations and the ancestry of the andamanese. *Hum. Genet.* **136**, 499–510 (2017).
13. Wojcik, G. L. *et al.* Genetic analyses of diverse populations improves discovery for complex traits. *Nature* **570**, 514–518 (2019).
14. Skoglund, P. *et al.* Genomic insights into the peopling of the Southwest Pacific. *Nature* **538**, 510–513 (2016).
15. Posth, C. *et al.* Language continuity despite population replacement in Remote Oceania. *Nat. Ecol. Evol.* **2**, 731–740 (2018).
16. Prüfer, K. *et al.* The complete genome sequence of a Neanderthal from the Altai Mountains. *Nature* **505**, 43–49 (2014).
17. Meyer, M. *et al.* A High-Coverage Genome Sequence from an Archaic Denisovan Individual. *Science* **338**, 222–226 (2012).
18. Waterson, R. H., Lander, E. S., Wilson, R. K., Sequencing, T. C. & Consortium, A. Initial sequence of the chimpanzee genome and comparison with the human genome. *Nature* **437**, 69–87 (2005).